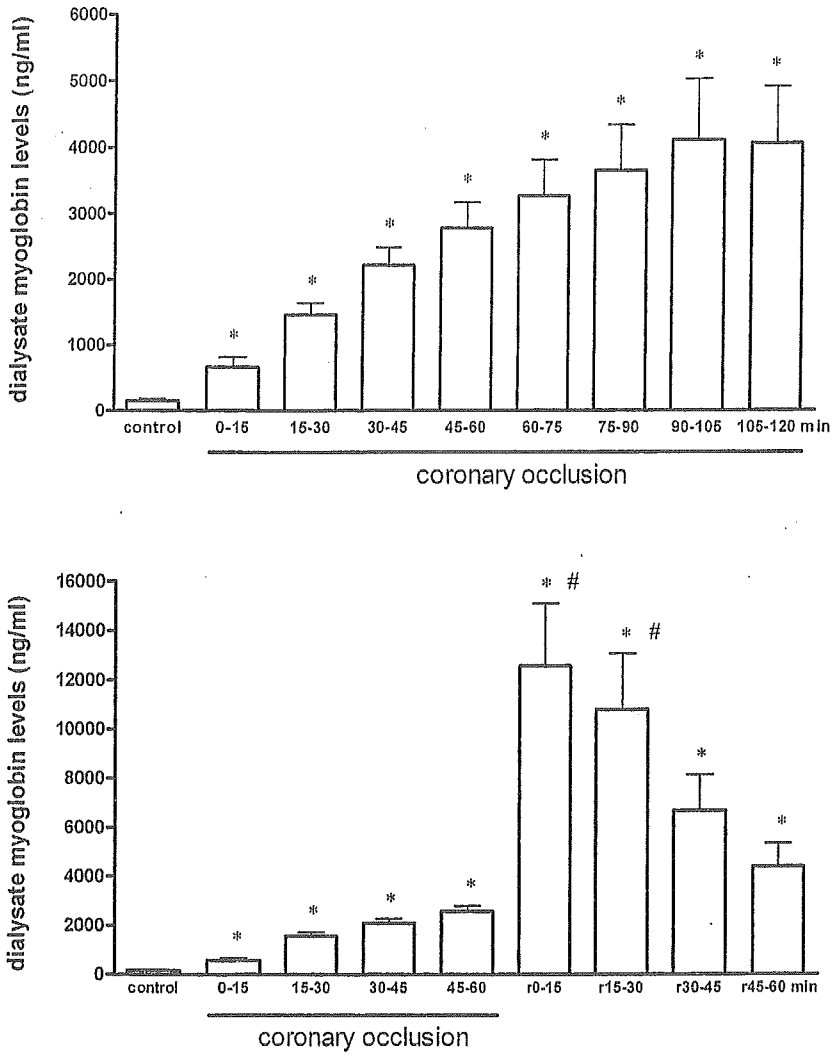

Fig. 4. Time courses of dialysate myoglobin levels during 120 min of ischemia (*top*) and 60 min of ischemia followed by 60 min of reperfusion (r, *bottom*). Values are means ± SE. $^{*}P < 0.05$ vs. control. $^{\#}P < 0.05$ vs. 45–60 min of occlusion.

dialysate myoglobin levels gradually decreased and reached 4,391 ± 879 ng/ml at 45–60 of reperfusion. At 0–15 min of reperfusion, dialysate lactate and glycerol levels were 3.27 ± 0.61 mmol/l and 242 ± 37.7 μmol/l, respectively. Dialysate lactate and glycerol levels remained unchanged at 0–15 min of reperfusion.

Time Course of Dialysate Myoglobin Levels During Local Administration of NaCN

Local administration of NaCN increased the dialysate myoglobin levels (Fig. 5). This increase was statistically significant compared with the control level at all collection periods during NaCN administration, except at 0–15 min. The maximum myoglobin level was comparable to that observed during 60 min of ischemia.

DISCUSSION

Using the dialysis technique in the in vivo rabbit heart, we observed myocardial interstitial myoglobin levels during myocardial ischemia and reperfusion. Our data demonstrated myoglobin release in the early stage of cardiac ischemia and its enhancement by reperfusion. We discuss here the time course of myocardial myoglobin release during coronary occlusion and after reperfusion.

We show for the first time that myoglobin release increases within 15 min of ischemia and continues to increase during 60 min of ischemia. However, significant changes in the blood myoglobin level occurred at 45–60 min of coronary occlusion. Our data suggest a contrast between blood and dialysate

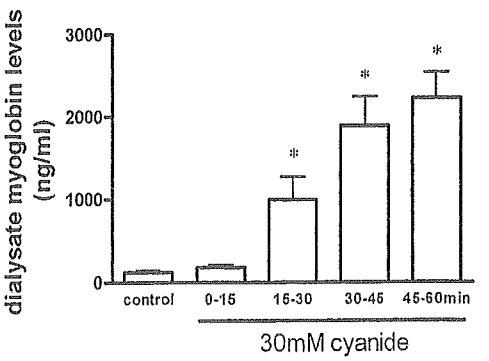

Fig. 5. Time course of dialysate myoglobin levels during local administration of sodium cyanide (30 mM). Values are means ± SE. $^{*}P < 0.05$ vs. control.

myoglobin levels during ischemia. The delay of the first appearance of myoglobin in the bloodstream is mainly due to the slow transport of myoglobin from the interstitial space into the bloodstream (20). Therefore, myoglobin concentration measured by cardiac microdialysis provides information regarding early release of cytosol protein into the interstitial space. Within the 15-min time resolution, this increase in myoglobin release was accompanied by increases in interstitial lactate. Dead space volume between the dialysis fiber and the sample microtube was identical for lactate, glycerol, and myoglobin. The currently accepted concept (20) is that leakage of anaerobic metabolites precedes macromolecular protein release during ischemia. Anaerobic metabolites accumulate and leak from the ischemic region within minutes via diffusion or transport (6, 12, 41). In contrast to low-molecular-weight metabolites, macromolecular proteins could be released into the interstitial space without cytosol accumulation of myoglobin, probably via bleb or altered permeability. Although sampling periods of 15 min are too long to enable us to distinguish the rate of release of lactate vs. myoglobin, our data at least suggest that cellular metabolic derangement is involved in membrane disruption for myoglobin release.

Myocardial injury caused by ischemia-reperfusion is associated with membrane phospholipid degradation, which is thought to underlie disruption of the cell membrane (27). Glycerol is an end product of membrane phospholipid degradation and has been used to study membrane phospholipid degradation after cerebral ischemia and seizures (12). In the present study, dialysate glycerol was examined as a potential marker for membrane phospholipid degradation in myocardial ischemia and reperfusion. We observed increases in dialysate glycerol levels during 15–60 min of ischemia but not during reperfusion. In general, phospholipid degradation is accentuated during reperfusion (27). Therefore, dialysate glycerol is not suitable as an index of membrane phospholipid degradation, and the release of glycerol from membrane phospholipid degradation might be too small to allow detection in blood-perfused heart.

Early change of cytosol myoglobin was detected by immunofluorescence after occlusion of the coronary artery (16, 25). Histochemical studies demonstrated that intracellular diffusion of cytosol myoglobin into the nuclei and mitochondria was evident as early as 0.5 h after coronary artery occlusion (17, 25). Our data demonstrate early loss of cytosol myoglobin into the interstitial space. Release of cytosol protein is caused by membrane damage via alteration of permeability or bleb formation. Blebs appeared on the cell surfaces, and the cell began to swell within 10–20 min of ATP depletion in a glia cell line or hepatocytes (13, 24). Furthermore, NMR spectroscopy suggested that sarcolemmal membranes are gradually permeabilized to large molecules by ischemia (3). These alterations of sarcolemmal membranes might be involved in early release of myoglobin during the myocardial ischemia. Our method offers extremely fast and sensitive analysis of membrane injury in myocardial ischemia that is not evident by histological or blood analysis. Quantitative assessment of interstitial myoglobin levels could be performed independently of reperfusion cell injury and could be helpful in devising various myocardial preservation treatments.

We show that reperfusion markedly accelerates myoglobin release in the ischemic region. The interstitial myoglobin levels at 0–15 min of reperfusion were fivefold higher than those at 60–75 min of 120 min of coronary occlusion. During the reperfusion period, interstitial accumulated myoglobin might be washed out into the bloodstream (37). Therefore, the amount of released myoglobin at reperfusion could be markedly greater than the changes in interstitial myoglobin concentrations at reperfusion. Release of cytosolic protein resulted from a disruption of a sarcolemmal bleb or an enhancement of membrane permeability (5, 29, 35). Either condition may gain relevance during the reperfusion period. Thus the release of myoglobin during the reperfusion seems to serve as an index of disrupted sarcolemmal membrane.

Although the exact mechanisms of accelerated myoglobin release cannot be determined from the present study, our data suggest that substances induced during reperfusion differ from those induced during ischemia. Reperfusion enhanced myoglobin release but did not accelerate lactate or glycerol release in the interstitial space, whereas ischemia accompanied macromolecular myoglobin release as well as anaerobic metabolite release. Furthermore, in the previous studies, neither catecholamine nor acetylcholine release was accelerated by reperfusion in ischemic cardiac sympathetic and parasympathetic nerve endings (2, 14). During reperfusion, surviving myocardial cells and nerve terminals quickly recover aerobic metabolism and take up these accumulated substances, whereas myocardial cells have no capability of myoglobin uptake via the sarcolemmal membrane, leading to continued myoglobin release via the disrupted membrane. Reperfusion may enhance membrane permeability (5). Further disruption of membrane blebs may cause rupture of the membrane (29, 35). Alternatively, in isolated perfused rats, leakage of cytoplasmic enzymes during reoxygenation is accelerated by cardiac revived beating, because the cell membrane becomes fragile during the preceding anoxia (36). In either condition, reperfusion-induced breakdown of membrane phospholipids contributes to an alteration of permeability or bleb formation (27). Disruption of the membrane phospholipid bilayer is likely to play a role in myoglobin release from the cyotosome into the interstitial spaces.

In the present study, we demonstrate that loss of cytosol myoglobin occurs during myocardial ischemia and reperfusion and might be involved in the outcome and pathophysiology of the ischemic heart. Loss of cytosol myoglobin may precede, at least in part, histological evidence of necrosis and occur in the remaining viable myocardium that is not necrotic (11). In vertebrate heart, myoglobin is involved in the transport of oxygen from the sarcolemma to the mitochondria (42). Recent studies from myoglobin knockout mice indicate that myoglobin contributes to the scavenging of bioactive nitric oxide (NO) or oxygen radicals during ischemia-reperfusion (9, 10). NO production and/or oxidant injury occur during the reperfusion period. In hearts lacking myoglobin, changes in NO and oxidative stress have a much larger impact on the maintenance of vascular tone and cardiac function (44). Similarly, in myoglobin knockout mice, loss of cytosol myoglobin may be involved in the delayed restoration of cardiac contractility in the postischemic region.

There are several limitations to the present study. First, with application of the dialysis technique to the heart, we had to perform this experiment as an acute surgical preparation. Probe implantation and/or surgical preparation might affect the con-

centration of myocardial interstitial myoglobin. To examine the effect of probe implantation and/or surgery, we performed the preliminary experiment on brief occlusion (3 min). Three minutes of coronary occlusion did not alter dialysate myoglobin levels. Furthermore, to confirm whether the dialysate myoglobin level reflects myocardial damage evoked by ischemia or hypoxia, we tested the effect of local NaCN administration on dialysate myoglobin levels: with NaCN, we found increases in dialysate myoglobin levels similar to the increase evoked by myocardial ischemia. Therefore, we believe that dialysate myoglobin levels reflect the release of myoglobin evoked by ischemia as well as by chemical hypoxia. The absolute myoglobin level might be affected by implantation and/or surgical preparation. However, it is possible to estimate myoglobin release from relative changes in myoglobin levels.

Second, in the present study, myocardial interstitial myoglobin levels during coronary occlusion and reperfusion were determined regionally. We implanted the dialysis probe in the midwall of the left ventricle. When the dialysis probe was implanted in the subendocardial zone, it is likely that subendocardial ischemia was much more severe than in the midwall, where the sampling was performed. Actually, subendocardial lactate was significantly greater than epicardial lactate during severe ischemia in the anesthetized dogs (6). Further studies are warranted concerning the influence of the ischemic area (subendocardial or marginal zone) on its myocardial interstitial myoglobin levels.

In summary, this microdialysis study in an ischemic animal model shows that coronary occlusion induced myoglobin release in minutes. Micromolecular metabolite (lactate) and macromolecular protein (myoglobin) increased during the first 15 min of ischemia. Reperfusion markedly enhanced myoglobin release without increases in lactate or glycerol levels. Elevation of myoglobin release represents an increase in sarcolemmal permeability or bleb formation during ischemia and reperfusion. Massive disruption of myocardial membrane occurs immediately after ischemia and is markedly accelerated by reperfusion. The dialysis technique permits more concise in vivo monitoring of myocardial membrane disruption during ischemia and reperfusion separately.

GRANTS

This study was supported by the Program for Promotion of Fundamental Studies in Health Science of the Organization for Pharmaceutical Safety and Research by grants-in-aid for scientific research from the Ministry of Education, Science.

REFERENCES

1. **Akiyama T, Yamazaki T, and Ninomiya I.** In vivo monitoring of myocardial interstitial norepinephrine by dialysis technique. *Am J Physiol Heart Circ Physiol* 261: H1643–H1647, 1991.
2. **Akiyama T, Yamazaki T, and Ninomiya I.** Differential regional response of myocardial interstitial noradrenaline levels to coronary occlusion. *Cardiovasc Res* 27: 817–822, 1993.
3. **Askenasy N, Vivi A, Tassini M, Navon G, and Farkas DL.** NMR spectroscopic characterization of sarcolemmal permeability during myocardial ischemia and reperfusion. *J Mol Cell Cardiol* 33: 1421–1433, 2001.
4. **Block MI, Said JW, Siegel RJ, and Fishbein MC.** Myocardial myoglobin following coronary artery occlusion. An immunohistochemical study. *Am J Pathol* 111: 374–379, 1983.
5. **Camilleri JP, Joseph D, Amat D, and Fabiani JN.** Impaired sacrolemmal membrane permeability in reperfused ischemic myocardium. Ultrastructual tracer study. *Virchows Arch* 388: 69–76, 1980.
6. **Delyani JA and Van Wylen GDL.** Endocardial and epicardial interstitial purines and lactate during graded ischemia. *Am J Physiol Heart Circ Physiol* 266: H1019–H1026, 1994.
7. **Dominici R, Infusino I, Valente C, Moraschineli I, and Franzini C.** Plasma or serum samples: measurements of cardiac troponin T and of other analytes compared. *Clin Chem Lab Med* 42: 945–951, 2004.
8. **Farb A, Kolodgie FD, Jones RM, Jenkins M, and Virmani R.** Early detection and measurement of experimental myocardial infarcts with horseradish peroxidase. *J Mol Cell Cardiol* 25: 343–353, 1993.
9. **Flögel U, Gödecke A, Klotz LO, and Schrader J.** Role of myoglobin in the antioxidant defense of the heart. *FASEB J* 18: 1156–1158, 2004.
10. **Flögel U, Merx MW, Gödecke A, Decking UKM, and Schrader J.** Myoglobin: a scavenger of bioactive NO. *Proc Natl Acad Sci USA* 98: 735–740, 2001.
11. **Heyndrickx GR, Amano J, Kenna T, Fallon JT, Patrick TA, Manders WT, Rogers GG, Rosendorff C, and Vatner SF.** Creatine kinase release not associated with myocardial necrosis after short periods of coronary artery occlusion in conscious baboons. *J Am Coll Cardiol* 6: 1299–1303, 1985.
12. **Hillered L, Valtysson J, Enblad P, and Persson L.** Interstitial glycerol as a marker for membrane phospholipid degradation in the acutely injured human brain. *J Neurol Neurosurg Psychiatry* 64: 486–491, 1998.
13. **Jurkowitz-Alexander MS, Altschuld RA, Hohl CM, Johnson JD, McDonald JS, Simmonds TD, and Horrocks LA.** Cell swelling, blebbing, and death are dependent on ATP depletion and independent of calcium during chemical hypoxia in a glial cell line (ROC-1). *J Neuorchem* 59: 344–352, 1992.
14. **Kawada T, Yamazaki T, Akiyama T, Sato T, Shishido T, Inagaki M, Sugimachi M, and Sunagawa K.** Differential acetylcholine release mechanisms in the ischemic and non-ischemic myocardium. *J Mol Cell Cardiol* 32: 405–414, 2000.
15. **Kennergren C, Nyström B, Nyström U, Berglin E, Larsson G, Mantovani V, Lönnroth P, and Hamberger A.** In situ detection of myocardial infarction in pig by measurements of asparate aminotransferase (ASAT) activity in the interstitial fluid. *Scand Cardiovasc J* 31: 343–349, 1997.
16. **Kent SP.** Diffusion of myoglobin in the diagnosis of early myocardial ischemia. *Lab Invest* 46: 265–270, 1982.
17. **Kent SP.** Intracellular diffusion of myoglobin. A manifestation of early cell injury in myocardial ischemia in dogs. *Arch Pathol Lab Med* 108: 827–830, 1984.
18. **Laperche T, Steg PG, Dehoux M, Benessiano J, Grollier G, Aliot E, Mossard JM, Aubry P, Coisne D, Hanssen M, and Iliou MC.** A study of biochemical markers of reperfusion early after thrombolysis for acute myocardial infarction. The PERM Study Group Prospective Evaluation of Reperfusion Markers. *Circulation* 92: 2079–2088, 1995.
19. **Le Quellec A, Dupin S, Genissel P, Savin S, Marchand B, and Houin G.** Microdialysis probes calibration: gradient and tissue dependent changes in no net flux and reverse dialysis methods. *J Pharmacol Toxicol Methods* 33: 11–16, 1995.
20. **Mair J.** Tissue release of cardiac markers: from physiology to clinical applications. *Clin Chem Lab Med* 37: 1077–1084, 1999.
21. **Matsumura K, Jeremy RW, Schaper J, and Becker LC.** Progression of myocardial necrosis during reperfusion of ischemic myocardium. *Circulation* 97: 795–804, 1998.
22. **Miura T.** Does reperfusion induce myocardial necrosis? *Circulation* 82: 1070–1072, 1990.
23. **Nachlas MM and Shnitka TK.** Macroscopic identification of early myocardial infarcts by alterations in dehydrogenase activity. *Am J Pathol* 42: 379–405, 1963.
24. **Nieminen AL, Gores GJ, Wray BE, Tanaka Y, Herman B, and Lemasters JJ.** Calcium dependence of bleb formation and cell death in hepatocytes. *Cell Calcium* 9: 237–246, 1988.
25. **Nomoto K, Mori N, Miyamoto J, Shoji T, and Nakamura K.** Relationship between sarcolemmal damage and appearance of amorphous matrix densities in mitochondria following occlusion of coronary artery in rats. *Exp Mol Pathol* 51: 231–242, 1989.
26. **Ortmann C, Pfeiffer H, and Brinkmann B.** A comparative study on the immunohistochemical detection of early myocardial damage. *Int J Legal Med* 113: 215–220, 2000.
27. **Prasad MR, Popescu LM, Moraru II, Liu X, Maity S, Engelman RM, and Das DK.** Role of phospholipases A_2 and C in myocardial ischemic reperfusion injury. *Am J Physiol Heart Circ Physiol* 260: H877–H883, 1991.

28. **Remppis A, Scheffold T, Greten J, Haass M, Greten T, Kubler W, and Katus HA.** Intracellular compartmentation of troponin T: release kinetics after global ischemia and calcium paradox in the isolated perfused rat heart. *J Mol Cell Cardiol* 27: 793–803, 1995.
29. **Sage MD and Jennings RB.** Cytoskeletal injury and subsarcolemmal bleb formation in dog heart during in vitro total ischemia. *Am J Pathol* 133: 327–337, 1988.
30. **Sarrafzadeh AS, Sakowitz OW, Kiening KL, Benndorf G, Lanksch WR, and Unterberg AW.** Bedside microdialysis: a tool to monitor cerebral metabolism in subarachnoid hemorrhage patients? *Crit Care Med* 30: 1062–1070, 2002.
31. **Shindo T, Akiyama T, Yamazaki T, and Ninomiya I.** Increase in myocardial norepinephrine during a short period of coronary occlusion. *J Auton Nerv Syst* 48: 91–96, 1994.
32. **Shindo T, Akiyama T, Yamazaki T, and Ninomiya I.** Regional myocardial interstitial norepinephrine kinetics during coronary occlusion and reperfusion. *Am J Physiol Heart Circ Physiol* 270: H245–H251, 1996.
33. **Shirato C, Miura T, Ooiwa H, Toyofuku T, Wilborn WH, and Downey JM.** Tetrazolium artifactually indicates superoxide dismutase-induced salvage in reperfused rabbit heart. *J Mol Cell Cardiol* 21: 1187–1193, 1989.
34. **Spangenthal EJ and Ellis AK.** Cardiac and skeletal muscle myoglobin release after reperfusion of injured myocardium in dogs with systemic hypotension. *Circulation* 91: 2635–2641, 1995.
35. **Steenbergen C, Hill ML, and Jennings RB.** Volume regulation and plasma membrane injury in aerobic, anaerobic, and ischemic myocardium in vitro. Effects of osmotic cell swelling on plasma membrane integrity. *Circ Res* 57: 864–875, 1985.
36. **Takami H, Matsuda H, Kuki S, Nishimura M, Kawashima Y, Watari H, Furuya E, and Tagawa K.** Leakage of cytoplasmic enzymes from rat heart by the stress of cardiac beating after increase in cell membrane fragility by anoxia. *Pflügers Arch* 416: 144–150, 1990.
37. **Van der Laarse A, van der Wall EE, van den Pol RC, Vermeer F, Verheugt FW, Krauss XH, Bar FW, Hermens WT, Willems GW, and Simoons ML.** Rapid enzyme release from acutely infarcted myocardium after early thrombolytic therapy: washout or reperfusion damage? *Am Heart J* 115: 711–716, 1988.
38. **Van Kreel BK, van den Veen FH, Willems GM, and Hermens WT.** Circulatory models in assessment of cardiac enzyme release in dogs. *Am J Physiol Heart Circ Physiol* 264: H747–H757, 1993.
39. **Van Nieuwenhoven FA, Musters RJ, Post JA, Verkleij AJ, Van der Vusse GJ, and Glatz JF.** Release of proteins from isolated neonatal rat cardiomyocytes subjected to simulated ischemia or metabolic inhibition is independent of molecular mass. *J Mol Cell Cardiol* 28: 1429–1434, 1996.
40. **Wiener BJ.** *Statistical Principles in Experimental Design* (2nd ed.). New York: McGraw-Hill, 1971.
41. **Wikström G, Ronquist G, Nilsson S, Maripu E, and Waldenström A.** Continuous monitoring of energy metabolites using microdialysis during myocardial ischaemia in the pig. *Eur Heart J* 16: 339–347, 1995.
42. **Wittenberg JB and Wittenberg BA.** Myoglobin function reassessed. *J Exp Biol* 206: 2011–2020, 2003.
43. **Wu AH.** Biochemical markers of cardiac damage: from traditional enzymes to cardiac-specific proteins. IFCC Subcommittee on Standardization of Cardiac Markers (S-SCM). *Scand J Clin Lab Invest Suppl* 230: 74–82, 1999.
44. **Wunderlich C, Flögel U, Gödecke A, Heger J, and Schrader J.** Acute inhibition of myoglobin impairs contractility and energy state of iNOS-overexpressing hearts. *Circ Res* 92: 1352–1358, 2003.

Transplantation of Mesenchymal Stem Cells Improves Cardiac Function in a Rat Model of Dilated Cardiomyopathy

Noritoshi Nagaya, MD; Kenji Kangawa, PhD; Takefumi Itoh, MD; Takashi Iwase, MD; Shinsuke Murakami, MD; Yoshinori Miyahara, MD; Takafumi Fujii, MD; Masaaki Uematsu, MD; Hajime Ohgushi, MD; Masakazu Yamagishi, MD; Takeshi Tokudome, MD; Hidezo Mori, MD; Kunio Miyatake, MD; Soichiro Kitamura, MD

Background—Pluripotent mesenchymal stem cells (MSCs) differentiate into a variety of cells, including cardiomyocytes and vascular endothelial cells. However, little information is available about the therapeutic potency of MSC transplantation in cases of dilated cardiomyopathy (DCM), an important cause of heart failure.

Methods and Results—We investigated whether transplanted MSCs induce myogenesis and angiogenesis and improve cardiac function in a rat model of DCM. MSCs were isolated from bone marrow aspirates of isogenic adult rats and expanded ex vivo. Cultured MSCs secreted large amounts of the angiogenic, antiapoptotic, and mitogenic factors vascular endothelial growth factor, hepatocyte growth factor, adrenomedullin, and insulin-like growth factor-1. Five weeks after immunization, MSCs or vehicle was injected into the myocardium. Some engrafted MSCs were positive for the cardiac markers desmin, cardiac troponin T, and connexin-43, whereas others formed vascular structures and were positive for von Willebrand factor or smooth muscle actin. Compared with vehicle injection, MSC transplantation significantly increased capillary density and decreased the collagen volume fraction in the myocardium, resulting in decreased left ventricular end-diastolic pressure (11 ± 1 versus 16 ± 1 mm Hg, $P<0.05$) and increased left ventricular maximum dP/dt (6767 ± 323 versus 5138 ± 280 mm Hg/s, $P<0.05$).

Conclusions—MSC transplantation improved cardiac function in a rat model of DCM, possibly through induction of myogenesis and angiogenesis, as well as by inhibition of myocardial fibrosis. The beneficial effects of MSCs might be mediated not only by their differentiation into cardiomyocytes and vascular cells but also by their ability to supply large amounts of angiogenic, antiapoptotic, and mitogenic factors. (***Circulation*. 2005;112:1128-1135.**)

Key Words: myocytes ■ angiogenesis ■ heart failure ■ growth substances ■ transplantation

Despite advances in medical and surgical procedures, congestive heart failure remains a leading cause of cardiovascular morbidity and mortality.[1] Idiopathic dilated cardiomyopathy (DCM), a primary myocardial disease of unknown etiology characterized by a loss of cardiomyocytes and an increase in fibroblasts, is an important cause of heart failure.[2] Although myocyte mitosis and the presence of cardiac precursor cells in adult hearts have recently been reported,[3] the death of large numbers of cardiomyocytes results in the development of heart failure. Thus, restoring lost myocardium would be desirable for the treatment of DCM.

Mesenchymal stem cells (MSCs) are pluripotent, adult stem cells residing within the bone marrow microenvironment.[4] In contrast to their hematopoietic counterparts, MSCs are adherent and can be expanded in culture. MSCs can differentiate not only into osteoblasts, chondrocytes, neurons, and skeletal muscle cells but also into vascular endothelial cells[5] and cardiomyocytes.[6,7] In vitro, MSCs can be induced to differentiate into beating cardiomyocytes by 5-azacytidine treatment.[8] In vivo, MSCs directly injected into an infarcted heart have been shown to induce myocardial regeneration and improve cardiac function.[9] In addition, MSC implantation induces therapeutic angiogenesis in a rat model of hindlimb ischemia through vascular endothelial growth factor (VEGF) production by MSCs.[10,11] Myocardial blood flow abnormalities, even in the presence of angiographically normal coronary arteries, have been documented in patients with DCM.[12]

Received August 18, 2004; revision received April 28, 2005; accepted May 10, 2005.

From the Departments of Regenerative Medicine and Tissue Engineering (N.N., T.I., T.I., S.M.), Internal Medicine (N.N., M.Y., K.M.), Biochemistry (K.K., T.T.), and Cardiac Physiology (Y.M., T.F., H.M.), National Cardiovascular Center Research Institute, Osaka; the Cardiovascular Division (M.U.), Kansai Rosai Hospital, Hyogo; the Tissue Engineering Research Center (H.O.), National Institute of Advanced Industrial Science and Technology, Hyogo; and the Department of Cardiovascular Surgery (S.K.), National Cardiovascular Center, Osaka, Japan.

Reprint requests to Noritoshi Nagaya, MD, Department of Regenerative Medicine and Tissue Engineering, National Cardiovascular Center Research Institute, 5-7-1 Fujishirodai, Suita, Osaka 565-8565, Japan. E-mail nnagaya@ri.ncvc.go.jp

Circulation is available at http://www.circulationaha.org

DOI: 10.1161/CIRCULATIONAHA.104.500447

These findings raise the possibility that transplanted MSCs have beneficial effects on myocardial structure and function via myogenesis and angiogenesis. However, little information is available about the therapeutic potential of MSCs for DCM.

A unique model of myocarditis in the rat has been created by immunization with porcine cardiac myosin,[13] which results in severe heart failure characterized by increased cardiac fibrosis and left ventricular (LV) dilation.[14] Thus, the late phase of this model can serve as a model of DCM.

The purpose of this study was to investigate the following topics: (1) whether transplantation of MSCs induces myogenesis and angiogenesis, decreases collagen deposition in the myocardium, and thereby improves cardiac function in a rat model of DCM and (2) whether the beneficial effects of MSCs are mediated by their differentiation into cardiomyocytes and vascular cells and/or by their supplying angiogenic, antiapoptotic, and mitogenic factors.

Methods

Expansion of Bone Marrow MSCs

MSC expansion was performed according to previously described methods.[4] In brief, we humanely killed male Lewis rats and harvested bone marrow by flushing their femoral and tibial cavities with phosphate-buffered saline (PBS). Bone marrow cells were cultured in α-minimal essential medium supplemented with 10% fetal bovine serum and antibiotics. A small number of cells developed visible symmetric colonies by days 5 to 7. Nonadherent hematopoietic cells were removed, and the medium was replaced. The adherent, spindle-shaped MSC population expanded to $>5\times10^7$ cells within $\approx$4 to 5 passages after the cells were first plated.

Flow Cytometry

Cultured MSCs were analyzed by fluorescence-activated cell sorting (FACS) (FACScan flow cytometer, Becton Dickinson). Cells were incubated with fluorescein isothiocyanate (FITC)–conjugated mouse monoclonal antibodies against rat CD31 (clone TLD-3A12, Becton Dickinson), CD34 (clone ICO-115, Santa Cruz), CD45 (clone OX-1, Becton Dickinson), CD90 (clone OX-7, Becton Dickinson), vimentin (clone V9, Dako), and smooth muscle actin (SMA; clone 1A4, Dako). FITC-conjugated hamster anti-rat CD29 monoclonal antibody (clone Ha2/5, Becton Dickinson) and rabbit anti-rat c-Kit polyclonal antibody (clone C-19, Santa Cruz) were used. Isotype-identical antibodies served as controls.

Model of DCM

Male Lewis rats weighing 220 to 250 g (Japan SLC Inc, Hamamatsu, Japan) were used in this study. These isogenic rats served as donors and recipients of MSCs to simulate autologous implantation. DCM was produced by inducing experimental myocarditis, as described previously.[13,14] In brief, 1 mg (0.1 mL) of porcine heart myosin (Sigma) was mixed with an equal volume of Freund's complete adjuvant (Sigma) and injected into a footpad on days 1 and 7. Five weeks after immunization, these rats served as a model of heart failure due to DCM.

MSC Transplantation

In a preliminary experiment, we performed dose-response studies to obtain the maximal effects of cell transplantation. Because the effect of 10^6 MSCs was modest, we used 5×10^6 MSCs for transplantation. Five weeks after immunization, we injected a total of 5×10^6 MSCs/100 μL PBS, or PBS alone, into the myocardium at 10 points. In brief, the LV was divided into 3 levels (basal, middle, and apical). The basal and middle levels were each subdivided into 4 segments, and the apical level was subdivided into 2 segments. Injection into each segment was performed with a 27-gauge needle. Sham rats received intramyocardial injections of 100 μL PBS. This protocol resulted in the creation of 3 groups: DCM rats given MSCs (MSC-treated DCM group, n=10); DCM rats given PBS (untreated DCM group, n=10); and sham rats given PBS (sham group, n=10). The Animal Care Committee of the National Cardiovascular Center approved this experimental protocol.

Echocardiographic Studies

Echocardiographic studies were performed by an investigator, blinded to treatment allocation, at 5 weeks after immunization (before treatment) and 4 weeks after cell transplantation (after treatment). Two-dimensional, targeted M-mode tracings were obtained at the level of the papillary muscles with an echocardiographic system equipped with a 7.5-MHz transducer (HP Sonos 5500, Hewlett-Packard).[15] LV dimensions were measured according to the American Society for Echocardiology leading-edge method from at least 3 consecutive cardiac cycles. Fractional shortening was calculated as (LVDd−LVDs)/LVDd×100, where LVDd=LV diastolic dimension and LVDs=LV systolic dimension.

Hemodynamic Studies

Hemodynamic studies were performed 4 weeks after cell transplantation. A 1.5F micromanometer-tipped catheter (Millar Instruments) was inserted into the right carotid artery for measurement of mean arterial pressure.[16] Next, the catheter was advanced into the LV for measurement of LV pressure. Hemodynamic variables were measured with a pressure transducer (model P23 ID, Gould) connected to a polygraph. After completion of these measurements, the left and right ventricles were excised and weighed.

Histological Examination

To detect fibrosis in cardiac muscle, the LV myocardium (n=5 from each group) was fixed in 10% formalin, cut transversely, embedded in paraffin, and stained with Masson's trichrome. Transverse sections were randomly obtained from the 3 levels (basal, middle, and apical), and 20 randomly selected fields per section (n=60 per animal) were analyzed. After each field was scanned and computerized with a digital image analyzer (WinRoof, Mitani Co), collagen volume fraction was calculated as the sum of all areas containing connective tissue divided by the total area of the image.[15]

To detect capillaries in the myocardium, samples of harvested muscle (n=5 each) were embedded in OCT compound (Miles Scientific), snap-frozen in LN_2, cut into transverse sections, and stained for alkaline phosphatase by an indoxyltetrazolium method. Transverse sections were randomly obtained from the 3 levels (basal, middle, and apical), and 5 randomly selected fields per section (n=15 per animal) were analyzed. The number of capillaries was counted by light microscopy at a magnification of ×200. The number of capillaries in each field was averaged and expressed as the number of capillary vessels. These morphometric studies were performed by 2 examiners who were blinded to treatment assignment.

Assessment of Cell Differentiation

Suspended MSCs were labeled with fluorescent dyes with use of a PKH26 red fluorescent cell linker kit (Sigma), as reported previously.[17] Fluorescence-labeled MSCs were injected into the myocardium 5 weeks after immunization. Rats (n=5) were humanely killed 4 weeks after cell transplantation. LV samples were embedded in OCT compound, snap-frozen in LN_2, and cut into sections. Immunofluorescence staining was performed with monoclonal mouse anti-cardiac troponin T (Novo), anti-desmin (Dako), anti-connexin-43 (Sigma), polyclonal rabbit anti–von Willebrand factor (Dako), and monoclonal mouse SMA (Dako). FITC-conjugated IgG antibody (BD Pharmingen) was used as a secondary antibody. To perform quantitative analysis of the magnitude of MSC differentiation into cardiomyocytes, heart cells from each rat (n=5) were isolated by incubation in balanced salt solution containing 0.06% collagenase type II (Worthington Biochemical Co), as reported previously.[18] PKH26/troponin T double-positive cells were detected by FACS.

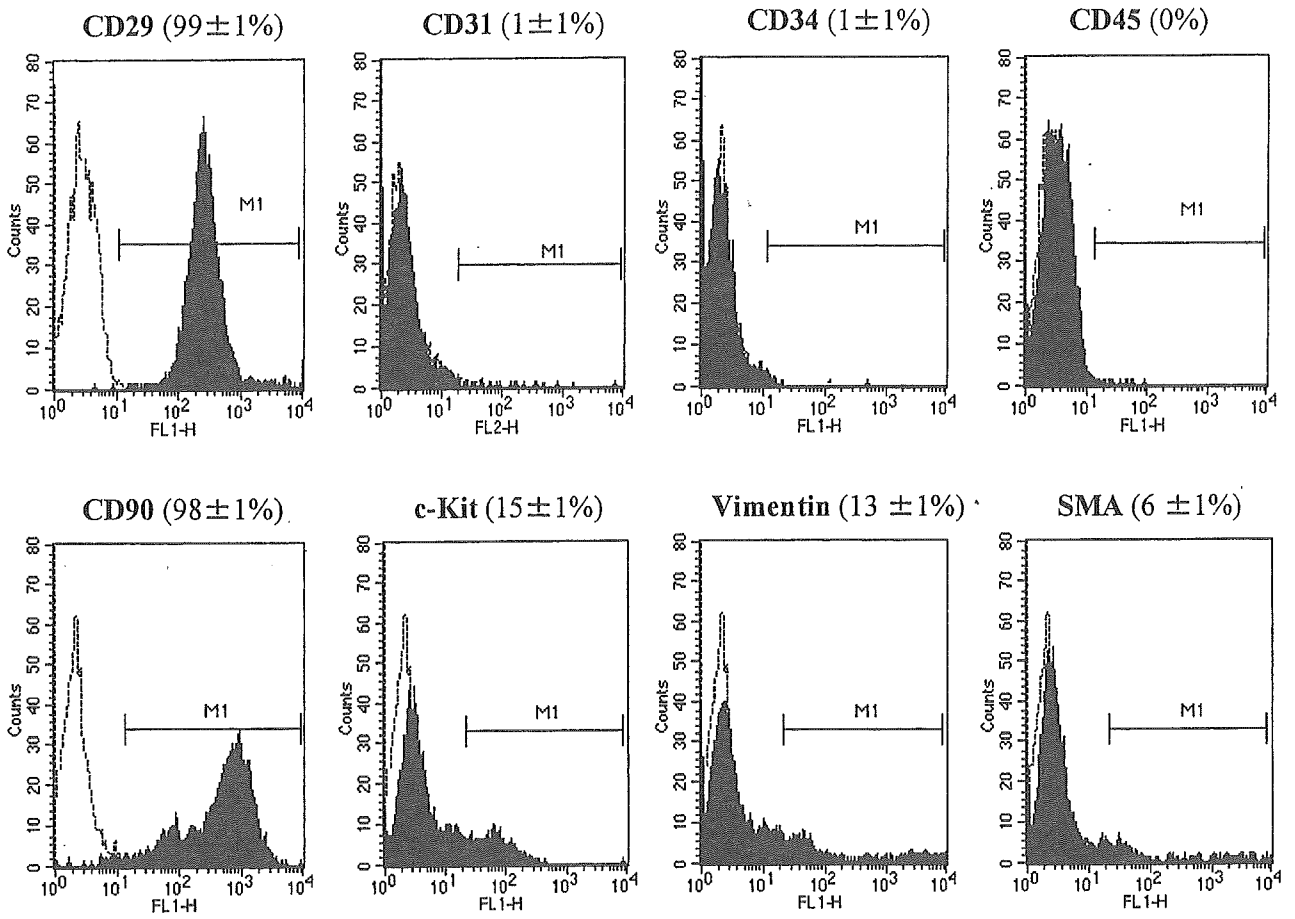

Figure 1. Flow-cytometric analysis of the adherent, spindle-shaped MSC population expanded to 4 to 5 passages. Most of the MSCs expressed CD29 and CD90, whereas they were negative for CD31, CD34, CD45, and SMA. Some of the cells were positive for c-Kit and vimentin.

Western Blot Analysis of Matrix Metalloproteinases

To identify the protein expression of matrix metalloproteinases (MMPs)-2 and -9, Western blotting was performed with rabbit polyclonal antibody raised against MMP-2 (Laboratory vision Co) and MMP-9 (Chemicon Co). The LV obtained from individual rats was used for comparison among the 3 groups (n=5 each). These samples were homogenized on ice in 0.1% Tween 20 homogenization buffer with a protease inhibitor. Then, 40 μg of protein was transferred into sample buffer, loaded on a 7.5% sodium dodecyl sulfate–polyacrylamide gel, and blotted onto a polyvinylidene fluoride membrane (Millipore Co). After being blocked for 120 minutes, the membrane was incubated with primary antibody at a dilution of 1:200. The membrane was incubated with peroxidase labeled with secondary antibody at a dilution of 1:1000. Positive protein bands were visualized with an ECL kit (Amersham) and measured by densitometry. Western blot analysis with a mouse polyclonal antibody raised against β-actin (Santa Cruz) was used as a protein loading control.

Assay for Angiogenic, Antiapoptotic, and Mitogenic Factors

To investigate whether MSCs produce angiogenic and growth factors, we measured VEGF, hepatocyte growth factor (HGF), insulin-like growth factor-1 (IGF-1), and adrenomedullin (AM) levels in conditioned medium 24 hours after medium replacement. VEGF, HGF, and IGF-1 were measured by enzyme immunoassay (VEGF immunoassay, R&D Systems Inc; rat HGF enzyme immunoassay, Institute of Immunology Co, Ltd; and active rat IGF-1 enzyme immunoassay, Diagnostic Systems Laboratories, Inc). AM level was measured with a radioimmunoassay kit (Shionogi Co), as reported previously.[19] The amounts of these products produced by MSCs were compared with those produced by bone marrow–derived mononuclear cells (MNCs) because MNCs have commonly been used for regenerative therapy.[19–21] There was no significant difference in cell viability between MSCs and MNCs 24 hours after seeding (88±5% versus 85±4% by trypan blue solution). In vivo, circulating levels of VEGF, HGF, IGF-1, and AM were measured before and 24 hours after administration of MSCs or vehicle (n=6 from each group).

Statistical Analysis

Numerical values are expressed as mean±SEM unless otherwise indicated. Comparisons of parameters between 2 groups were made with unpaired Student t test. Comparisons of parameters among 3 groups were made with a 1-way ANOVA, followed by the Scheffe multiple-comparison test. Comparisons of changes in parameters among the 3 groups were made by a 2-way ANOVA for repeated measures, followed by the Scheffe multiple-comparison test. A value of $P<0.05$ was considered significant.

Results

Characterization of Cultured MSCs

Most cultured MSCs expressed CD29 and CD90 (Figure 1). In contrast, the majority of MSCs were negative for CD31, CD34, CD45, and SMA. Some of the MSCs expressed c-Kit and vimentin.

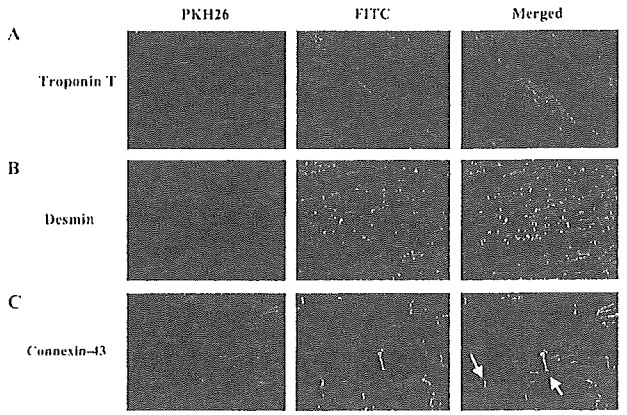

Figure 2. Differentiation of transplanted MSCs into cardiomyocytes. Transplanted MSCs were engrafted in the myocardium and stained for cardiac troponin T (A) and desmin (B). Engrafted MSCs also expressed connexin-43, a gap junction protein, at contact points with native cardiac myocytes (left arrow) and other transplanted cells (right arrow) (C). Magnification ×400.

Myogenesis and Angiogenesis Induced by MSCs

Red fluorescence–labeled MSCs were transplanted into the myocardium 5 weeks after immunization. Four weeks after transplantation, MSCs were engrafted into the myocardium (Figure 2). Immunofluorescence demonstrated that transplanted MSCs were positive for the cardiac markers cardiac troponin T and desmin (Figure 2). Transplanted MSCs also expressed connexin-43, a gap junction protein, at contact points with native cardiac myocytes as well as with MSCs. FACS analysis of isolated heart cells demonstrated that 8±1% of transplanted MSCs were double-positive for PKH26 and troponin T. These results suggest that a small number of transplanted MSCs can differentiate into cardiomyocytes.

Some transplanted MSCs formed vascular structures in the myocardium and were positive for von Willebrand factor (Figure 3A). Other MSCs were positive for SMA and participated in vessel formation as mural cells (Figure 3B). Alkaline phosphatase staining of the ischemic myocardium showed marked augmentation of neovascularization in the MSC-treated DCM group (Figures 4A–4C). Quantitative analysis demonstrated that capillary density was significantly

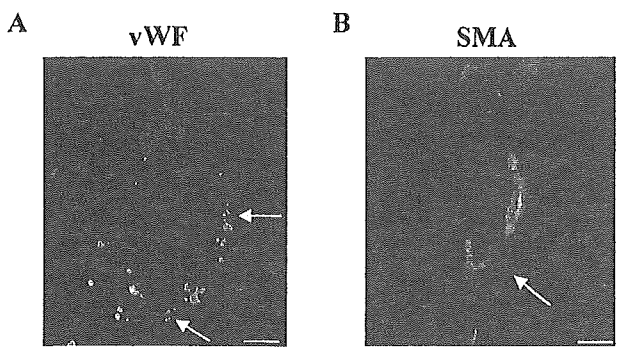

Figure 3. Differentiation of transplanted MSCs into vascular endothelial cells and smooth muscle cells. Some of the transplanted MSCs were positive for von Willebrand factor (vWF, A) and SMA (B) and formed vascular structures (A and B). Scale bars=10 μm.

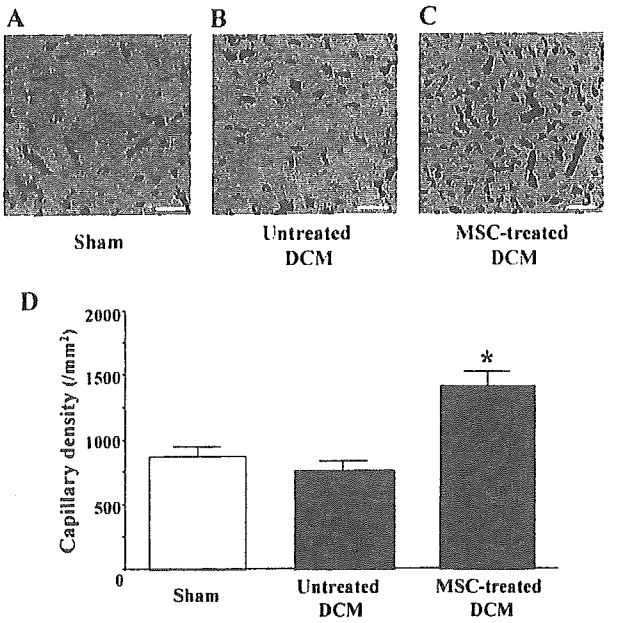

Figure 4. A–C, Representative samples of alkaline phosphatase staining of myocardium. Magnification, ×200. Scale bars=10 μm. D, Quantitative analysis of capillary density in the myocardium. Data are mean±SEM *P<0.05 vs untreated DCM group.

higher in the MSC-treated DCM group than in the untreated DCM group (Figure 4D).

Angiogenic, Antiapoptotic, and Mitogenic Factors Released From MSCs

After 24 hours of culture, MSCs secreted large amounts of angiogenic and antiapoptotic factors, including VEGF, HGF, and AM (Figure 5). Compared with MNCs that have commonly been used for regenerative therapy,[20–22] MSCs secreted 4-fold more VEGF and 5-fold more HGF. Similarly, MSCs secreted 6-fold more AM, an angiogenic and antiapoptotic peptide, compared with MNCs. MSCs also secreted a large amount, 10-fold greater than MNCs, of IGF-1, a growth hormone mediator for myocardial growth (Figure 5). Transplantation of MSCs significantly increased circulating VEGF (45.8±1.6 to 68.5±3.6 pg/mL, P<0.05), HGF (431.8±56.6 to 517.2±67.1 pg/mL, P<0.05), and AM (23.4±0.8 to 41.2±4.8 pg/mL, P<0.05) 24 hours after transplantation, although vehicle injection did not alter these parameters. Serum IGF-1 tended to increase after MSC transplantation (938.1±151.6 to 1063.5±116.9 pg/mL, P=NS), but this increase did not reach statistical significance.

Hemodynamic Effects of MSC Transplantation

Nine weeks after immunization, LV end-diastolic pressure showed a marked elevation in the untreated DCM group; this elevation was significantly attenuated in the MSC-treated DCM group (Figure 6A). LV maximum *dP/dt* was significantly lower in the untreated DCM group than in the sham group (Figure 6B). However, LV maximum *dP/dt* was significantly improved 4 weeks after MSC transplantation. There was no significant difference in heart rate or mean arterial pressure among the 3 groups (the Table). Echocardiographic studies demonstrated LV dysfunction and dilation

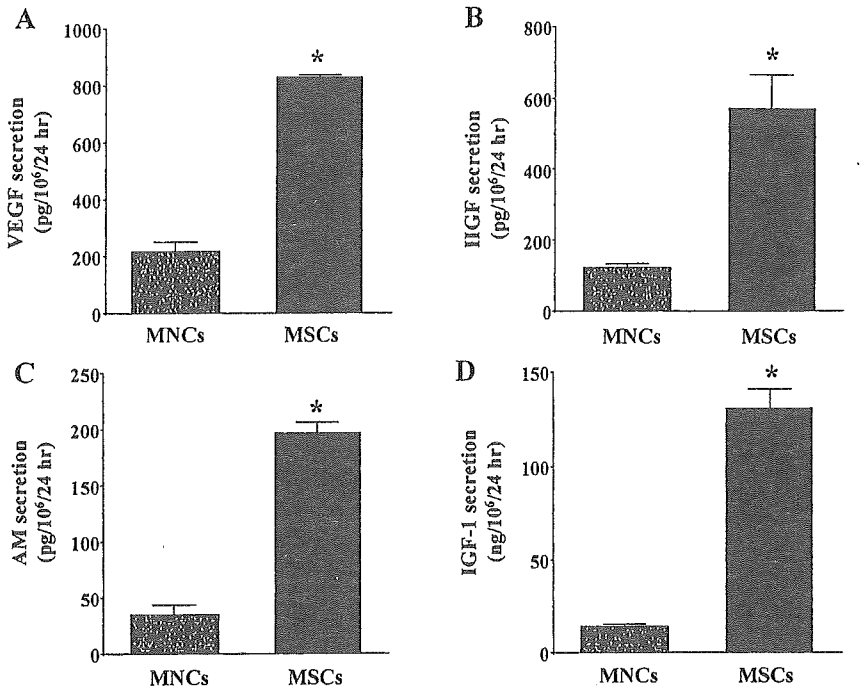

Figure 5. A–D, Angiogenic, antiapoptotic, and mitogenic factors produced by MSCs and bone marrow–derived MNCs). Compared with MNCs, MSCs secreted large amounts of VEGF, HGF, AM, and IGF-1. *$P<0.05$ vs MNCs.

in the untreated DCM group, as indicated by a decrease in percent fractional shortening and an increase in LV diastolic dimension (Figure 6C and 6D). However, MSC transplantation increased percent fractional shortening and inhibited the increase in LV diastolic dimension.

Reduction of Myocardial Fibrosis by MSC Transplantation

Masson's trichrome staining demonstrated modest myocardial fibrosis in the untreated DCM group (Figure 7A). However, MSC transplantation significantly attenuated the development of myocardial fibrosis. Quantitative analysis also demonstrated that the collagen volume fraction in the MSC-treated DCM group was significantly smaller than that in the untreated DCM group (Figure 7B). Western blot analysis showed that myocardial contents of MMP-2 and MMP-9 in the untreated DCM were significantly increased compared with those in the sham group (Figure 7C–E). However, the increases in MMP-2 and MMP-9 levels were attenuated by MSC transplantation, although the change in MMP-9 did not reach statistical significance.

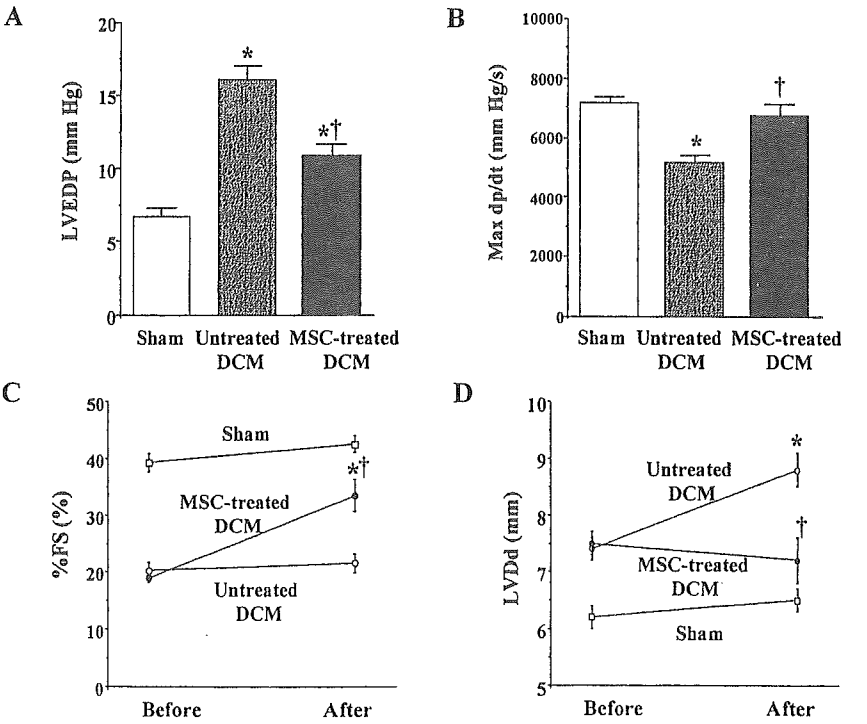

Figure 6. A and B, Effects of MSC transplantation on hemodynamic parameters. LVEDP indicates LV end-diastolic pressure; Max *dP/dt*, LV maximum *dP/dt*. Data are mean±SEM. *$P<0.05$ vs sham group; †$P<0.05$ vs untreated DCM group. C and D, Changes in echocardiographic parameters induced by MSC transplantation. %FS indicates LV fractional shortening. Data are mean±SEM *$P<0.05$ vs before transplantation; †$P<0.05$ vs the time-matched untreated DCM group.

Physiological Profiles of the 3 Experimental Groups

	Sham	Untreated DCM	MSC-Treated DCM
n	10	10	10
Body wt, g	421±8	372±4*	389±5*
LV wt/body wt, g/kg	1.91±0.05	2.18±0.06*	2.05±0.05
RV wt/body wt, g/kg	0.55±0.01	0.68±0.02*	0.60±0.03†
Heart rate, bpm	403±10	432±15	417±12
Mean arterial pressure, mm Hg	134±2	123±3	132±5

wt indicates weight; RV, right ventricle. Sham-operated rats were given vehicle only. The untreated DCM group included DCM rats treated with vehicle. The MSC-treated DCM group included DCM rats treated with MSCs. Data are mean±SEM.

*$P<0.05$ vs sham group; †$P<0.05$ vs untreated DCM group.

Discussion

In the present study, we have demonstrated the following effects of MSC transplantation in a rat model of DCM: (1) induction of myogenesis and angiogenesis; (2) differentiation of transplanted MSCs into cardiomyocytes, vascular endothelial cells, and smooth muscle cells; (3) secretion of large amounts of VEGF, HGF, AM, and IGF-1; (4) improvement of cardiac function and inhibition of ventricular remodeling; and (5) decrease in collagen volume fraction in the myocardium.

Earlier studies have shown that transplantation of MSCs improves cardiac function in experimental models of ischemic heart disease.[9,23] However, little information is available about the therapeutic potential of MSCs for chronic heart failure due to DCM. Previous studies have shown that porcine cardiac myosin-induced myocarditis progresses to a chronic phase resembling DCM.[13,14] Thus, we used this model 5 weeks after immunization as an example of experimental DCM.

In the present study, transplanted MSCs were engrafted into the myocardium in a rat model of DCM. Four weeks after transplantation, some of the engrafted MSCs were positively stained for cardiac troponin T and desmin. Transplanted MSCs also expressed connexin-43, a gap junction protein, at contact points with native cardiac myocytes as well as with MSCs. These results suggest that MSCs differentiate into cardiomyocytes in the myocardium and form connections with native cardiomyocytes in rats with DCM. Unlike earlier studies that have used a model of myocardial infarction,[7,9,23] we used a rat model of DCM to demonstrate the engraftment and cardiogenic differentiation of MSCs. Importantly, MSC transplantation improved cardiac function in these rats, as indicated by a significant decrease in LV end-diastolic pressure and an increase in LV dP/dt_{max}. Thus, the improvement in cardiac function may be a result of MSC-induced myocardial regeneration; however, further studies are necessary to investigate the mechanisms by which MSCs develop into cardiac myocyte–like cells.

Some of the transplanted MSCs were positive for a vascular endothelial cell marker and participated in vessel formation. MSC transplantation significantly increased capillary density in the myocardium. SMA staining revealed that MSCs differentiated into vascular smooth muscle cells, which play an important role in vessel maturation. Earlier studies have shown that transplantation of MNCs induces therapeutic angiogenesis in patients with limb ischemia or ischemic heart disease.[20–22] The angiogenic potential of MNCs is mediated at least in part by production by the cells of a variety of angiogenic factors.[24] Although MSCs have also been shown to produce VEGF,[10,25] there has been no study to compare their production between MSCs and MNCs. The present study demonstrated that MSCs secreted ≈4-fold more VEGF compared with MNCs. Furthermore, MSCs secreted large amounts of HGF and AM, potent angiogenic factors.[26–30] Taking these findings together, MSCs may contribute to neovascularization in the myocardium not only through their ability to generate capillary-like structures but also through growth factor–mediated paracrine regulation. Myocardial blood flow abnormalities have been documented in patients with heart failure caused by DCM.[12] Thus, it is possible that MSC-induced neovascularization contributes to improvement in cardiac function.

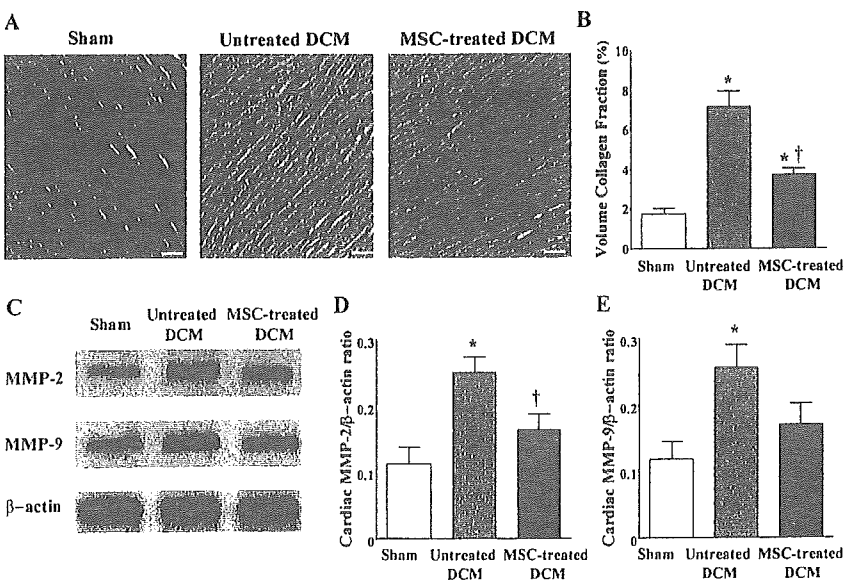

Figure 7. Effects of MSC transplantation on myocardial fibrosis. A, Photomicrographs show representative myocardial sections stained with Masson's trichrome. Scale bars=10 μm. B, Quantitative analysis demonstrated that the collagen volume fraction in the MSC-treated DCM group was significantly smaller than that in the untreated DCM group. C, Representative Western blots for MMPs-2 and -9 and β-actin in the heart. D and E, Quantitative analysis of cardiac tissue contents of MMP-2 and -9. Data are mean±SEM *$P<0.05$ vs sham group; †$P<0.05$ vs untreated DCM group.

HGF has not only angiogenic but also cardioprotective effects, including antiapoptotic, mitogenic, and antifibrotic activities.[26,27] *HGF* gene transfer into the myocardium improves myocardial function and geometry.[28] In particular, the antifibrotic effects of HGF through inhibition of transforming growth factor-β expression is beneficial for heart failure. Cultured MSCs secreted a large amount of HGF. In vivo, transplantation of MSCs slightly increased plasma HGF in rats. It significantly attenuated the development of myocardial fibrosis in a rat model of DCM. These results suggest that MSC-derived HGF may contribute to improvements in cardiac function partly through its antifibrotic effects.

MSCs also produced AM, a potent vasodilator and cardioprotective peptide.[29] We have shown that AM prevents cardiomyocyte apoptosis through the phosphatidylinositol 3-kinase/Akt–dependent pathway[16] and that it has potent angiogenic effects.[30] AM inhibits proliferation of cardiac fibroblasts through the cAMP-dependent pathway.[31] Administration of AM inhibits LV remodeling and improves cardiac function in heart failure.[32–34] In the present study, cultured MSCs secreted a large amount of AM in vitro. In vivo, transplantation of MSCs markedly increased plasma AM level. Taken together, these findings suggest that MSCs may exert their cardioprotective effects through AM-mediated paracrine regulation.

IGF-1, a growth hormone mediator, plays an important role in myocardial and skeletal muscle growth.[35,36] Administration of IGF-1 improves cardiac function after myocardial infarction through enhancement of myocardial growth.[37] Its protective and antiapoptotic properties have been demonstrated in different models of myocardial ischemia.[38] Furthermore, IGF-1 exerts Ca^{2+}-dependent, positive inotropic effects through a phosphatidylinositol 3-kinase–dependent pathway.[39] Interestingly, the present study demonstrated that MSCs secreted significant amounts of IGF-1 in vitro, 10-fold greater than MNCs. These findings raise the possibility that MSC-derived IGF-1 may participate in myocardial growth and enhancement of myocardial contractility in a rat model of DCM.

MMPs also play a crucial role in extracellular remodeling in heart failure.[40] In fact, pharmacological inhibition of MMP activities prevents progressive LV remodeling in an animal model of heart failure.[41] In the present study, cardiac MMP-2 and MMP-9 were increased in rats with DCM, which is consistent with recent findings in patients with heart failure.[40,42] Interestingly, MSC transplantation attenuated the increases in cardiac MMP-2 and MMP-9 in a rat model of DCM. Although the underlying mechanisms remain unclear, MSC transplantation may influence extracellular remodeling in heart failure.

The present study has some limitations. First, immunohistochemical evidence suggests differentiation of MSCs into cardiomyocytes, vascular endothelial cells, and smooth muscle cells. However, further studies are necessary to convincingly demonstrate differentiation of MSCs into a specific cell type. Second, the model of DCM used in this study was an injury model, and the effects of treatment may be related to attenuation of the injury rather than to the established cardiomyopathy. Nonetheless, the experiment was performed 5 to 9 weeks after myosin injection, by which time inflammatory changes were hardly observed and had been replaced by fibrosis.[43]

Conclusions

MSC transplantation improved cardiac function in a rat model of DCM, possibly through induction of myogenesis and angiogenesis, as well as by inhibition of myocardial fibrosis. The beneficial effects of MSCs may be mediated at least in part by their differentiation into cardiomyocytes and vascular cells and by their ability to supply large amounts of angiogenic, antiapoptotic, and mitogenic factors. Thus, MSC transplantation has potential as a new therapeutic strategy for the treatment of DCM.

Acknowledgments

This work was supported by research grants for cardiovascular disease (16C-6) and Human Genome Tissue Engineering 009 from the Ministry of Health, Labor and Welfare; the Industrial Technology Research Grant Program in '03 from the New Energy and Industrial Technology Development Organization of Japan; a research grant from the Japan Cardiovascular Research Foundation; and Promotion of Fundamental Studies in Health Science of the Organization for Pharmaceutical Safety and Research of Japan.

References

1. Cohn JN. The management of chronic heart failure. *N Engl J Med.* 1996;335:490–498.
2. Dec GW, Fuster V. Idiopathic dilated cardiomyopathy. *N Engl J Med.* 1994;331:1564–1575.
3. Beltrami AP, Urbanek K, Kajstura J, Yan SM, Finato N, Bussani R, Nadal-Ginard B, Silvestri F, Leri A, Beltrami CA, Anversa P. Evidence that human cardiac myocytes divide after myocardial infarction. *N Engl J Med.* 2001;344:1750–1757.
4. Pittenger MF, Mackay AM, Beck SC, Jaiswal RK, Douglas R, Mosca JD, Moorman MA, Simonetti DW, Craig S, Marshak DR. Multilineage potential of adult human mesenchymal stem cells. *Science.* 1999;284:143–147.
5. Reyes M, Dudek A, Jahagirdar B, Koodie L, Marker PH, Verfaillie CM. Origin of endothelial progenitors in human postnatal bone marrow. *J Clin Invest.* 2002;109:337–346.
6. Toma C, Pittenger MF, Cahill KS, Byrne BJ, Kessler PD. Human mesenchymal stem cells differentiate to a cardiomyocyte phenotype in the adult murine heart. *Circulation.* 2002;105:93–98.
7. Mangi AA, Noiseux N, Kong D, He H, Rezvani M, Ingwall JS, Dzau VJ. Mesenchymal stem cells modified with Akt prevent remodeling and restore performance of infarcted hearts. *Nat Med.* 2003;9:1195–1201.
8. Makino S, Fukuda K, Miyoshi S, Konishi F, Kodama H, Pan J, Sano M, Takahashi T, Hori S, Abe H, Hata J, Umezawa A, Ogawa S. Cardiomyocytes can be generated from marrow stromal cells in vitro. *J Clin Invest.* 1999;103:697–705.
9. Shake JG, Gruber PJ, Baumgartner WA, Senechal G, Meyers J, Redmond JM, Pittenger MF, Martin BJ. Mesenchymal stem cell implantation in a swine myocardial infarct model: engraftment and functional effects. *Ann Thorac Surg.* 2002;73:1919–1925.
10. Al-Khaldi A, Al-Sabti H, Galipeau J, Lachapelle K. Therapeutic angiogenesis using autologous bone marrow stromal cells: improved blood flow in a chronic limb ischemia model. *Ann Thorac Surg.* 2003;75:204–209.
11. Al-Khaldi A, Eliopoulos N, Martineau D, Lejeune L, Lachapelle K, Galipeau J. Postnatal bone marrow stromal cells elicit a potent VEGF-dependent neoangiogenic response in vivo. *Gene Ther.* 2003;10:621–629.
12. Parodi O, De Maria R, Oltrona L, Testa R, Sambuceti G, Roghi A, Merli M, Belingheri L, Accinni R, Spinelli F, Pellegrini A, Baroldi G. Myocardial blood flow distribution in patients with ischemic heart disease or dilated cardiomyopathy undergoing heart transplantation. *Circulation.* 1993;88:509–522.
13. Kodama M, Zhang S, Hanawa H, Saeki M, Inomata T, Suzuki K, Koyama S, Shibata A. Effects of 15-deoxyspergualin on experimental autoimmune giant cell myocarditis of the rat. *Circulation.* 1995;91:1116–1122.
14. Watanabe K, Ohta Y, Nakazawa M, Higuchi H, Hasegawa G, Naito M, Fuse K, Ito M, Hirono S, Tanabe N, Hanawa H, Kato K, Kodama M, Aizawa Y. Low dose carvedilol inhibits progression of heart failure in rats with dilated cardiomyopathy. *Br J Pharmacol.* 2000;130:1489–1495.

15. Nagaya N, Uematsu M, Kojima M, Ikeda Y, Yoshihara F, Shimizu W, Hosoda H, Hirota Y, Ishida H, Mori H, Kangawa K. Chronic administration of ghrelin improves left ventricular dysfunction and attenuates development of cardiac cachexia in rats with heart failure. *Circulation.* 2001;104:1430–1435.
16. Okumura H, Nagaya N, Itoh T, Okano I, Hino J, Mori K, Tsukamoto Y, Ishibashi-Ueda H, Miwa S, Tambara K, Toyokuni S, Yutani C, Kangawa K. Adrenomedullin infusion attenuates myocardial ischemia/reperfusion injury through the phosphatidylinositol 3-kinase/Akt-dependent pathway. *Circulation.* 2004;109:242–248.
17. Messina LM, Podrazik RM, Whitehill TA, Ekhterae D, Brothers TE, Wilson JM, Burkel WE, Stanley JC. Adhesion and incorporation of lacZ-transduced endothelial cells into the intact capillary wall in the rat. *Proc Natl Acad Sci U S A.* 1992;89:12018–12022.
18. Harada M, Itoh H, Nakagawa O, Ogawa Y, Miyamoto Y, Kuwahara K, Ogawa E, Igaki T, Yamashita J, Masuda I, Yoshimasa T, Tanaka I, Saito Y, Nakao K. Significance of ventricular myocytes and nonmyocytes interaction during cardiocyte hypertrophy: evidence for endothelin-1 as a paracrine hypertrophic factor from cardiac nonmyocytes. *Circulation.* 1997;96:3737–3744.
19. Ohta H, Tsuji T, Asai S, Sasakura K, Teraoka H, Kitamura K, Kangawa K. A simple immunoradiometric assay for measuring the entire molecules of adrenomedullin in human plasma. *Clin Chim Acta.* 1999;287:B131–B143.
20. Murohara T, Ikeda H, Duan J, Shintani S, Sasaki K, Eguchi H, Onitsuka I, Matsui K, Imaizumi T. Transplanted cord blood-derived endothelial precursor cells augment postnatal neovascularization. *J Clin Invest.* 2000; 105:1527–1536.
21. Tateishi-Yuyama E, Matsubara H, Murohara T, Ikeda U, Shintani S, Masaki H, Amano K, Kishimoto Y, Yoshimoto K, Akashi H, Shimada K, Iwasaka T, Imaizumi T. Therapeutic Angiogenesis using Cell Transplantation (TACT) Study Investigators. Therapeutic angiogenesis for patients with limb ischaemia by autologous transplantation of bone-marrow cells: a pilot study and a randomised controlled trial. *Lancet.* 2002;360:427–435.
22. Tse HF, Kwong YL, Chan JK, Lo G, Ho CL, Lau CP. Angiogenesis in ischaemic myocardium by intramyocardial autologous bone marrow mononuclear cell implantation. *Lancet.* 2003;4:47–49.
23. Min JY, Sullivan MF, Yang Y, Zhang JP, Converso KL, Morgan JP, Xiao YF. Significant improvement of heart function by cotransplantation of human mesenchymal stem cells and fetal cardiomyocytes in postinfarcted pigs. *Ann Thorac Surg.* 2002;74:1568–1575.
24. Kamihata H, Matsubara H, Nishiue T, Fujiyama S, Tsutsumi Y, Ozono R, Masaki H, Mori Y, Iba O, Tateishi E, Kosaki A, Shintani S, Murohara T, Imaizumi T, Iwasaka T. Implantation of bone marrow mononuclear cells into ischemic myocardium enhances collateral perfusion and regional function via side supply of angioblasts, angiogenic ligands, and cytokines. *Circulation.* 2001;104:1046–1052.
25. Kinnaird T, Stabile E, Burnett MS, Lee CW, Barr S, Fuchs S, Epstein SE. Marrow-derived stromal cells express genes encoding a broad spectrum of arteriogenic cytokines and promote in vitro and in vivo arteriogenesis through paracrine mechanisms. *Circ Res.* 2004;94:678–685.
26. Nakamura T, Nishizawa T, Hagiya M, Seki T, Shimonishi M, Sugimura A, Tashiro K, Shimizu S. Molecular cloning and expression of human hepatocyte growth factor. *Nature.* 1989;342:440–443.
27. Nakamura T, Mizuno S, Matsumoto K, Sawa Y, Matsuda H, Nakamura T. Myocardial protection from ischemia/reperfusion injury by endogenous and exogenous HGF. *J Clin Invest.* 2000;106:1511–1519.
28. Li Y, Takemura G, Kosai K, Yuge K, Nagano S, Esaki M, Goto K, Takahashi T, Hayakawa K, Koda M, Kawase Y, Maruyama R, Okada H, Minatoguchi S, Mizuguchi H, Fujiwara T, Fujiwara H. Postinfarction treatment with an adenoviral vector expressing hepatocyte growth factor relieves chronic left ventricular remodeling and dysfunction in mice. *Circulation.* 2003;107:2499–2506.
29. Kitamura K, Kangawa K, Kawamoto M, Ichiki Y, Nakamura S, Matsuo H, Eto T. Adrenomedullin: a novel hypotensive peptide isolated from human pheochromocytoma. *Biochem Biophys Res Commun.* 1993;192:553–560.
30. Tokunaga N, Nagaya N, Shirai M, Tanaka E, Ishibashi-Ueda H, Harada-Shiba M, Kanda M, Ito T, Shimizu W, Tabata Y, Uematsu M, Nishigami K, Sano S, Kangawa K, Mori H. Adrenomedullin gene transfer induces therapeutic angiogenesis in a rabbit model of chronic hind limb ischemia: benefits of a novel nonviral vector, gelatin. *Circulation.* 2004;109:526–531.
31. Tsuruda T, Kato J, Kitamura K, Kawamoto M, Kuwasako K, Imamura T, Koiwaya Y, Tsuji T, Kangawa K, Eto T. An autocrine or a paracrine role of adrenomedullin in modulating cardiac fibroblast growth. *Cardiovasc Res.* 1999;43:958–967.
32. Nishikimi T, Yoshihara F, Horinaka S, Kobayashi N, Mori Y, Tadokoro K, Akimoto K, Minamino N, Kangawa K, Matsuoka H. Chronic administration of adrenomedullin attenuates transition from left ventricular hypertrophy to heart failure in rats. *Hypertension.* 2003;42:1034–1041.
33. Nakamura R, Kato J, Kitamura K, Onitsuka H, Imamura T, Cao Y, Marutsuka K, Asada Y, Kangawa K, Eto T. Adrenomedullin administration immediately after myocardial infarction ameliorates progression of heart failure in rats. *Circulation.* 2004;110:426–431.
34. Nagaya N, Satoh T, Nishikimi T, Uematsu M, Furuichi S, Sakamaki F, Oya H, Kyotani S, Nakanishi N, Goto Y, Masuda Y, Miyatake K, Kangawa K. Hemodynamic, renal, and hormonal effects of adrenomedullin infusion in patients with congestive heart failure. *Circulation.* 2000;101:498–503.
35. Fuller J, Mynett JR, Sugden PH. Stimulation of cardiac protein synthesis by insulin-like growth factors. *Biochem J.* 1992;282:85–90.
36. Florini JR, Ewton DZ, Coolican SA. Growth hormone and the insulin-like growth factor system in myogenesis. *Endocr Rev.* 1996;17:481–517.
37. Cittadini A, Stromer H, Katz SE, Clark R, Moses AC, Morgan JP, Douglas PS. Differential cardiac effects of growth hormone and insulin-like growth factor-1 in the rat: a combined in vivo and in vitro evaluation. *Circulation.* 1996;93:800–809.
38. Li Q, Li B, Wang X, Leri A, Jana KP, Liu Y, Kajstura J, Baserga R, Anversa P. Overexpression of insulin-like growth factor-1 in mice protects from myocyte death after infarction, attenuating ventricular dilation, wall stress, and cardiac hypertrophy. *J Clin Invest.* 1997;100:1991–1999.
39. von Lewinski D, Voss K, Hulsmann S, Kogler H, Pieske B. Insulin-like growth factor-1 exerts Ca^{2+}-dependent positive inotropic effects in failing human myocardium. *Circ Res.* 2003;92:169–176.
40. Thomas CV, Coker ML, Zellner JL, Handy JR, Crumbley AJ 3rd, Spinale FG. Increased matrix metalloproteinase activity and selective upregulation in LV myocardium from patients with end-stage dilated cardiomyopathy. *Circulation.* 1998;97:1708–1715.
41. Spinale FG, Coker ML, Krombach SR, Mukherjee R, Hallak H, Houck WV, Clair MJ, Kribbs SB, Johnson LL, Peterson JT, Zile MR. Matrix metalloproteinase inhibition during the development of congestive heart failure: effects on left ventricular dimensions and function. *Circ Res.* 1999;85:364–376.
42. Spinale FG, Coker ML, Heung LJ, Bond BR, Gunasinghe HR, Etoh T, Goldberg AT, Zellner JL, Crumbley AJ. A matrix metalloproteinase induction/activation system exists in the human left ventricular myocardium and is upregulated in heart failure. *Circulation.* 2000;102:1944–1949.
43. Kodama M, Matsumoto Y, Fujiwara M, Zhang SS, Hanawa H, Itoh E, Tsuda T, Izumi T, Shibata A. Characteristics of giant cells and factors related to the formation of giant cells in myocarditis. *Circ Res.* 1991;69:1042–1050.

CLINICAL PERSPECTIVE

Transplantation of stem or progenitor cells has the potential to improve and restore cardiac function. To date, experimenters investigating the possible therapeutic effects of stem cells in the heart have used models of infarction, and little information is available about the therapeutic potential of cell transplantation for heart failure due to dilated cardiomyopathy. In the present study, we demonstrated that transplantation of stem cells improved cardiac function in a model of myocarditis. We found evidence that stem cells may work to improve heart function by both myogenesis and angiogenesis while inhibiting myocardial fibrosis. Based on our data, part of the mechanism for this improvement may occur through the action of stem cells as a source of growth factors and cytokines in the heart. This study supports the overall notion that mesenchymal stem cells transplanted into the failing heart have potential as a new therapeutic strategy for the treatment of dilated cardiomyopathy.

Available online at www.sciencedirect.com
SCIENCE DIRECT®
Neuroscience Letters 388 (2005) 61–64
Neuroscience Letters
www.elsevier.com/locate/neulet

Contribution of catechol *O*-methyltransferase to the removal of accumulated interstitial catecholamines evoked by myocardial ischemia

Yosuke Kuroko [a], Takafumi Fujii [a], Toji Yamazaki [b,*], Tsuyoshi Akiyama [b], Kozo Ishino [a], Shunji Sano [a], Hidezo Mori [b]

[a] *Department of Cardiovascular Surgery, Okayama University Graduate School of Medicine and Dentistry, Okayama 700-8558 Japan*
[b] *Department of Cardiac Physiology, National Cardiovascular Center Research Institute, 5-7-1 Fujishiro-dai, Suitâ, Osaka 565-8565 Japan*

Received 7 May 2005; received in revised form 15 June 2005; accepted 16 June 2005

Abstract

Catechol *O*-methyltransferase (COMT) plays an important role for clearance of high catecholamine levels. Although myocardial ischemia evokes similar excessive catecholamine accumulation, it is uncertain whether COMT activity is involved in the removal of accumulated catecholamines evoked by myocardial ischemia. We examined how COMT activity affects myocardial catecholamine levels during myocardial ischemia and reperfusion. We implanted a dialysis probe into the left ventricular myocardial free wall and measured dialysate catecholamines levels in anesthetized rabbits. Dialysate catecholamine levels served as an index of myocardial interstitial catecholamine levels. We introduced myocardial ischemia by 60 min occlusion of the main coronary artery. The ischemia-induced dialysate catecholamines levels were compared with and without the pretreatment with entacapone (COMT inhibitor, 10 mg/kg, i.p.). Acute myocardial ischemia progressively increased dialysate catecholamine levels. Acute myocardial ischemia increased dialysate norepinephrine (NE) levels (20,453 ± 7186 pg/ml), epinephrine (EPI) levels (1724 ± 706 pg/ml), and dopamine (DA) levels (1807 ± 800 pg/ml) at the last 15 min of coronary occlusion. Inhibition of COMT activity by entacapone augmented the ischemia-induced NE levels (54,306 ± 6618 pg/ml), EPI levels (2681 ± 567 pg/ml), and DA (3551 ± 710 pg/ml) levels at the last 15 min of coronary occlusion. Myocardial ischemia evoked NE, EPI, and DA accumulation in the myocardial interstitial space. The inhibition of COMT activity augmented these increments in NE, EPI, and DA. These data suggest that cardiac COMT activity influences on the removal of accumulated catecholamine during myocardial ischemia.

Keywords: Catecholamine; Microdialysis; Myocardial infarction; Heart; Catechol *O*-methyltransferase

Myocardial ischemia evokes an excessive norepinephrine (NE) accumulation in the myocardial interstitial space [2,15]. Interstitial NE is largely removed by NE transport into the sympathetic nerve endings and metabolized to dihydroxyphenylglycol (DHPG) via monoamine oxidase (MAO) [6,22]. The remainder spills over into the coronary sinus [6]. However, during myocardial ischemia, two important NE removing systems are impaired. Myocardial ischemia reduces coronary flow, which abolishes NE spillover. Furthermore, membrane NE transport is dependent on the Na^+ gradient between the extracellular and intracellular spaces. During ischemia, NE uptake is blocked and outward NE transport through the uptake$_1$ carrier is induced by the reduced Na^+ gradient [17]. Thus, production of DHPG via MAO is inhibited by myocardial ischemia [1]. Up to now, little has been known about the role of catechol *O*-methyltransferase (COMT) in the removal of interstitial NE. Catechol *O*-methyltransferase has been believed to be operative only at high concentrations of NE via NE infusion [12]. An excessive NE accumulation in the myocardial ischemia was similar to NE levels in

* Corresponding author. Tel.: +81 6 6833 5012x2379; fax: +81 6 6872 8092.
E-mail address: yamazaki@ri.ncvc.go.jp (T. Yamazaki).

0304-3940/$ – see front matter © 2005 Elsevier Ireland Ltd. All rights reserved.
doi:10.1016/j.neulet.2005.06.031

intravenous NE infusion. Therefore, this NE removal system may be the sole mechanism that decreases myocardial interstitial NE.

Recent study has demonstrated that myocardial ischemia is associated with a pronounced increase in the concentration of endogenous NE, epinephrine (EPI), dopamine (DA) in the myocardial interstitial space [14]. These accumulated catecholamines may be a candidate of substrate of COMT. However, in most experiments on COMT activity, isoprenaline was used as the substrate of COMT [11,19] since it is not a substrate for neuronal uptake and MAO activity. Furthermore, data on isolated perfused lungs suggest that the affinity of COMT activity for *O*-methylation differed among the three amines [3]. It is uncertain whether COMT activity is involved in the removal of accumulated interstitial catecholamines evoked by myocardial ischemia.

In the present study, the possibility that the concentration of these three catecholamines in the myocardial interstitial space was affected by COMT activity was examined in anesthetized myocardial ischemic rabbits. With the use of dialysis technique, a dialysis probe was implanted into the left ventricle free wall perfused by the main branch of left circumflex coronary artery (LCX) to measure myocardial interstitial catecholamines levels in the ischemic region and dialysate catecholamines levels were compared in the absence and presence of COMT inhibitor.

Animal care proceeded in strict accordance with the *Guide for the Care and Use of Laboratory Animals* published by the US National Institutes of Health (NIH Publication No. 85-23, revised 1996). Adult male Japanese white rabbits (2.5–3.2 kg) were anesthetized with pentobarbital sodium (30–35 mg/kg i.v.). The level of anesthesia was maintained with a continuous intravenous infusion of pentobarbital sodium (1–2 mg/kg/h). The rabbits were intubated and ventilated with room air mixed with oxygen. Heart rate, arterial pressure, and electrocardiogram were simultaneously monitored with a data recorder. The fifth or sixth rib on the left side was partially removed to expose the heart. A 4–0 silk suture was passed around the main branch of LCX, to act as the occluder for later coronary occlusion. With a fine guiding needle, a dialysis probe was implanted in the region perfused by LCX of the left ventricular wall. Judging from changes in the color of the ventricular wall during a brief coronary occlusion, the dialysis probe was located in the midst of the ischemic region. Heparin sodium (100 IU/Kg) was administered intravenously to prevent blood coagulation.

The dialysate NE, EPI, and DA levels were measured as an index of myocardial interstitial NE, EPI, and DA levels, respectively. A dialysis fiber (8 mm length, 0.31 mm o.d., and 0.20 mm i.d.; PAN-1200 50,000 molecular weight cutoff, Asahi Chemical Japan) was glued at both ends of a polyethylene tube. The dialysis probe was perfused with Ringer's solution at a perfusion speed of 2 μl/min. Dialysate NE level was measured by the first HPLC after removing interfering compounds by the alumina procedure [23]. Dialysate EPI and DA levels were measured by direct injection into the second HPLC [18].

After control sampling, we occluded the main branch of LCX for 60 min and then released the occluder. The 15-min dialysate samples were collected before, during and after 60 min LCX occlusion. In vehicle group, we administered saline intraperitoneally as vehicle 120 min before control sampling. After control sampling, we observed the time course of dialysate NE, EPI, and DA levels from the ischemic region during 60 min of coronary occlusion and 15 min of reperfusion. To elucidate the role of COMT activity in the ischemia-induced changes in myocardial interstitial NE EPI, and DA levels, we compared dialysate NE, EPI, and DA levels in the ischemic region with those levels after injection of COMT inhibitor. We administered intraperitoneally the COMT inhibitor entacapone (10 mg/kg; Orion-Pharma, Espoo, Finland) 120 min before control sampling. Entacapone was dissolved in phosphate buffered saline, the pH of the solution was adjusted to 7.4, and the dose of entacapone was determined based on the dose used in the earlier preliminary experiments [7,8].

Changes in the dialysate NE levels in the vehicle and the pretreatment with entacapone are shown in Fig. 1. In the vehicle group, dialysate NE level averaged from six rabbits was 52 ± 12 pg/ml in the control. During 60 min coronary occlusion, dialysate NE levels markedly increased. The dialysate NE levels reached up to 400 times the control levels during the last 15 min of 60 min coronary occlusion. After release of the occluder, dialysate NE levels rapidly decreased to 3473 ± 735 pg/ml, although their levels were higher than those in the control. In the presence of entacapone, dialysate NE levels also markedly increased during 60 min coronary occlusion. The dialysate NE levels reached up to 1000 times the control levels during the last 15 min of 60 min coronary occlusion. These increases in dialysate NE levels at 15–60 min of coronary occlusion were significantly enhanced by entacapone whereas entacapone did not change dialysate NE levels in the control (51 ± 16 pg/ml) or at 0–15 min of

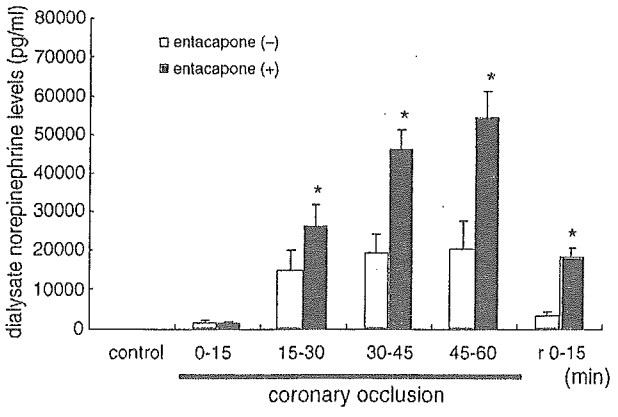

Fig. 1. Dialysate norepinephrine levels before, during and after 60 min-coronary occlusion. Values are mean ± S.E. ($n = 6$). $^*P < 0.05$ vs. concurrent value of vehicle group.

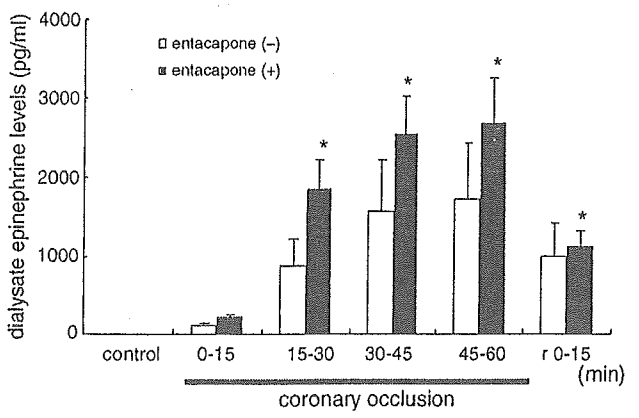

Fig. 2. Dialysate epinephrine levels before, during and after 60 min-coronary occlusion. Values are mean ± S.E. ($n = 6$). $^{*}P < 0.05$ vs. concurrent value of vehicle group.

coronary occlusion. Dialysate NE levels decreased by reperfusion, but remained higher than those in vehicle group. Thus, COMT activity for NE removal was operative in ischemic and reperfusion periods. Entacapone augmented peak NE levels to 160% of vehicle group.

Dialysate EPI levels were below the detectable level in the control. After coronary occlusion, dialysate EPI levels gradually increased and reached 1724 ± 706 pg/ml at 45–60 min of occlusion (Fig. 2). Peak EPI levels during the ischemia were one-twentieth of NE levels during the ischemic period. In the presence of entacapone, dialysate EPI levels were below the detectable level in the control. Dialysate EPI levels gradually increased during coronary occlusion and reached 2681 ± 567 pg/ml at 45–60 min of occlusion. In the presence of entacapone, dialysate EPI levels at 15–60 min of the ischemia were higher than those in the vehicle group. Entacapone augmented peak EPI levels by 50% of vehicle group.

Dialysate DA levels were below the detectable level in the control and at 0–15 min of ischemia. After 15 min of occlusion, dialysate DA levels gradually increased and reached 1807 ± 800 pg/ml at 45–60 min of occlusion (Fig. 3). Peak DA levels during the ischemia were one-twentieth of NE

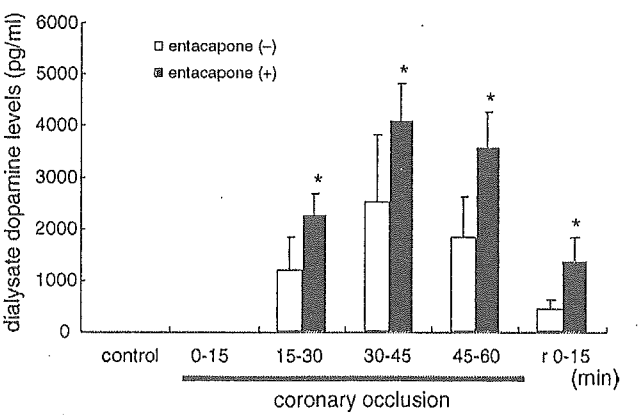

Fig. 3. Dialysate dopamine levels before, during and after 60 min-coronary occlusion. Values are mean ± S.E. ($n = 6$). $^{*}P < 0.05$ vs. concurrent value of vehicle group.

levels during the ischemia. In the presence of entacapone, dialysate DA levels were below the detectable level in the control and at 0–15 min of the occlusion. Dialysate DA levels gradually increased during 15–60 min of the ischemia and reached 3351 ± 710 pg/ml at 45–60 min of occlusion. In the presence of entacapone, dialysate DA levels at 15–60 min of the ischemia were higher than those in the vehicle group. Entacapone augmented peak DA levels by 100% of vehicle group.

Myocardial ischemia induced a progressive increase of interstitial catecholamines. The rank order of the amount of catecholamine release was NE much greater than EPI or DA, with this rank order remaining unchanged before, during and after myocardial ischemia. These findings are in line with those reported by Lameris et al. [14] studied the time course of myocardial interstitial catecholamine levels during myocardial ischemia. The measurement of overall content in the left ventricle free wall was performed in dogs [13] and the in vitro ratio of EPI/NE or DA/NE was similar to our result. Therefore, the rank order may reflect the ratio of overall catecholamine content in the left ventricle free wall.

In the resting state and early period (0–15 min) of ischemia, COMT does not appear to contribute to the removal of myocardial interstitial catecholamine levels. In the mid-late period of ischemia, COMT contributes to the inactivation of high myocardial interstitial catecholamine levels evoked by ischemia. The rank order of the amount of neurotransmitter release was NE much greater than EPI or DA. From percentage increase of catecholamine by entacapone, the rank order of COMT activity for removal of catecholamines was considered to be NE greater than DA greater than EPI. On the other hand, when catecholamines were infused in the isolated rat heart, the metabolism of the catecholamines by COMT differs: DA = NE less than EPI [9]. These data suggest that contribution of COMT to removal of accumulated catecholamines depends on the types of amines and the amount of accumulated catecholamine. In the absence of catecholamine spill over and MAO activity, COMT might constitutes one of major pathways of catecholamine metabolism in ischemic heart. Alternatively all three catecholamines are taken up and then metabolized by COMT at the extraneuronal tissues [4,10]. Uptake and *O*-methylation may handle three catecholamines in a different manner.

Up to now, little has been known about the role of cardiac COMT activity in the removal of accumulated interstitial catecholamine. In the isolated perfused rat, Carlsson et al. [5], demonstrated that marked NE release was paralleled by an increasing extraneuronal inactivation of released NE. Accumulated catecholamine in myocardial interstitial space is involved in the pathophysiology of ischemic heart disease [16,21]. Therefore, these data suggest that inhibition of COMT activity deteriorates myocardial ischemic injury via enhanced catecholamine accumulation. In contrast to this hypothesis, Valenza et al. [20], demonstrated that the inhibition of COMT (by nitecapone) improved the mechanical function of the heart during ischemia-reperfusion injury. In

the present study, we did not measure myocardial contractile function or biochemical markers. Future work should concentrate on these aspects of COMT action during myocardial ischemia.

Acknowledgement

This work was supported by Grands-in-Aid for scientific research (15590787) from the Ministry of Education, Culture, Sports, Science and Technology. The authors thank Orion-Pharma (Espoo, Finland) for the supply of entacapone.

References

[1] T. Akiyama, T. Yamazaki, Myocardial interstitial norepinephrine and dihydroxyphenylglycol levels during ischemia and reperfusion, Cardiovasc. Res. 49 (2001) 78–85.
[2] T. Akiyama, T. Yamazaki, I. Ninomiya, Differential regional responses of myocardial interstitial noradrenaline levels to coronary occlusion, Cardiovasc. Res. 27 (1993) 817–822.
[3] L.J. Bryan-Lluka, S.R. O'Donnell, Dopamine and adrenaline, but not isoprenaline, are substrates for uptake and metabolism in isolated perfused lungs of rats, Naunyn Schmiedebergs Arch. Pharmacol. 346 (1992) 20–26.
[4] C. Burgdorf, A. Dendorfer, T. Kurz, E. Schömig, I. Stolting, F. Schutte, G. Richardt, Role of neuronal KATP channels and extraneuronal monoamine transported on norepinephrine overflow in a model of myocardial low flow ischemia, J. Pharmacol. Exp. Ther. 309 (2004) 42–48.
[5] L. Carlsson, T. Abrahamsson, O. Almgren, Release of noradrenaline in myocardial ischemia-importance of local inactivation by neuronal and extraneuronal mechanisms, J. Cardiovasc Pharmacol. 8 (1986) 545–553.
[6] G. Eisenhofer, J.J. Smolich, H.S. Cox, M.D. Esler, Neuronal reuptake of norepinephrine and production of dihydroxyphenylglycol by cardiac sympathetic nerve in the anesthetized dog, Circulation 84 (1991) 1354–1363.
[7] T. Fujii, T. Yamazaki, T. Akiyama, S. Sano, H. Mori, In vivo assessment of catechol *O*-methyltransferase activity in rabbit skeletal muscle, Auton. Neurosci. 111 (2004) 140–143.
[8] T. Fujii, T. Yamazaki, T. Akiyama, S. Sano, H. Mori, Extraneuronal enzymatic degradation of myocardial norepinephrine in the ischemic region, Cardiovasc. Res. 64 (2004) 125–131.
[9] M. Grohmann, The activity of the neuronal and extraneuronal catecholamine metabolizing enzymes of the perfused rat heart, Naunyn Schmiedebergs Arch. Pharmacol. 336 (1987) 139–147.
[10] M. Grohmann, U. Trendelenburg, The handling of five catecholamines by the extraneuronal *O*-methylating system of the rat heart, Naunyn Schmiedebergs Arch. Pharmacol. 329 (1985) 264–270.
[11] M. Inoue, K. Hifumi, K. Kurahashi, M. Fujiwara, Impairment of the extraneuronal *O*-methylating system of isoproterenol by stop-flow ischemia in the perfused rat heart, J. Pharmacol. Exp. Ther. 242 (1987) 1086–1089.
[12] L.L. Iversen, P.J. The uptake of catechol amines at high perfusion concentrations in the rat isolated heart: a novel catechol amine uptake process, Br. J. Pharmacol. 25 (1965) 18–33.
[13] W.R. Kaufman, B.I. Jugdutt, Left ventricular catecholamines during acute myocardial infarction in the dog, Can. J. Physiol. Pharmacol. 65 (1987) 172–178.
[14] T.W. Lameris, S. deZeeuw, G. Alberts, F. Boomsma, D.J. Duncker, P.D. Verdouw, A.J. Man in't Veld, A.H. van den Meiracker, Time course and mechanism of myocardial catecholamine release during transient ischemia in vivo, Circulation 101 (2000) 2645–2650.
[15] P. Mertes, K. El-Abbassi, Y. Jabpin, C. Michel, B. Beck, G. Pinelli, J. Carteaux, J. Villemot, C. Burlet, Consequences of coronary occlusion on changes in regional interstitial myocardial neuropeptide Y and norepinephrine concentrations, J. Mol. Cell. Cardiol. 28 (1996) 1995–2004.
[16] W.J. Penny, The deleterious effects of myocardial catecholamines on cellular electrophysiology and arrhythmias during ishaemia and reperfusion, Eur. Heart J. 5 (1984) 960–973.
[17] A. Schömig, T. Kurz, G. Richardt, E. Schömig, Neuronal sodium homeostatis and axoplasmic amine concentration determine calcium-independent noradrenaline release in normoxic and ischemic rat heart, Circ. Res. 63 (1988) 214–226.
[18] N. Tokunaga, T. Yamazaki, T. Akiyama, H. Mori, Detection of 3-methoxy-4-hydroxyphenylglycol in rabbit skeletal muscle microdialysate, J. Cnromatogr. B. 798 (2003) 163–166.
[19] U. Trendelenburg, H. Fleig, L.J. Bryan, H. Bönisch, The extraneuronal compartments for the distribution of isoprenaline in the rat heart, Naunyn Schmiedebergs Arch. Pharmacol. 324 (1983) 169–179.
[20] M. Valenza, E. Sarbinova, L. Packer, S. Khwaja, J. Catudioc, Nitecapone protects the Langendorff perfused heart against ischemia-reperfusion injury, Biochem. Mol. Biol. Int. 29 (1993) 443–449.
[21] A.P. Waldenström, A.C. Hjalmarson, L. Thornell, A possible role of noradrenaline in the development of myocardial infarction. An experimental study in the isolated rat heart, Am. Heart. J. 95 (1978) 43–51.
[22] T. Yamazaki, T. Akiyama, H. Kitagawa, T. Kawada, K. Sunagawa, Dialysate dihydroxyphenylglycol as a window for in situ axoplasmic norepinephrine disposition, Neurochem. Int. 38 (2001) 287–292.
[23] T. Yamazaki, T. Akiyama, T. Shindo, Routine high-performance liquid chromatographic determination of the myocardial interstitial norepinephrine, J. Chromatogr. B. 670 (1995) 328–331.

Acta Crystallographica Section F
Structural Biology and Crystallization Communications
ISSN 1744-3091

Youssef Ben Ammar,[a] Soichi Takeda,[b] Mitsuaki Sugawara,[c] Masashi Miyano,[c] Hidezo Mori[b] and Shigeo Wakabayashi[a]*

[a]Department of Molecular Physiology, National Cardiovascular Center Research Institute, Fujishiro-dai 5-7-1, Suita, Osaka 565-8565, Japan, [b]Department of Cardiac Physiology, National Cardiovascular Center Research Institute, Fujishiro-dai 5-7-1, Suita, Osaka 565-8565, Japan, and [c]Structural Biophysics Laboratory, RIKEN Harima Institute at SPring-8, Kouto, Mikazuki, Sayo, Hyogo 679-5148, Japan

Correspondence e-mail: wak@ri.ncvc.go.jp

Received 18 August 2005
Accepted 27 September 2005
Online 30 September 2005

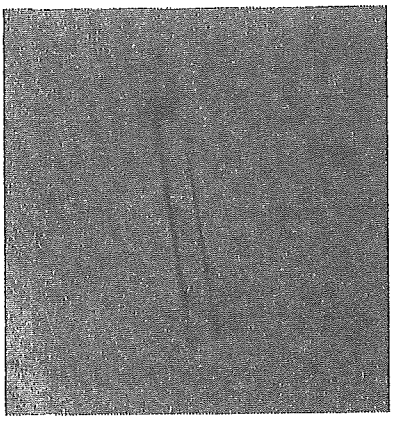

Crystallization and preliminary crystallographic analysis of the human calcineurin homologous protein CHP2 bound to the cytoplasmic region of the Na^+/H^+ exchanger NHE1

Calcineurin homologous protein (CHP) is a Ca^{2+}-binding protein that directly interacts with and regulates the activity of all plasma-membrane Na^+/H^+-exchanger (NHE) family members. In contrast to the ubiquitous isoform CHP1, CHP2 is highly expressed in cancer cells. To understand the regulatory mechanism of NHE1 by CHP2, the complex CHP2–NHE1 (amino acids 503–545) has been crystallized by the sitting-drop vapour-diffusion method using PEG 3350 as precipitant. The crystals diffract to 2.7 Å and belong to a tetragonal space group, with unit-cell parameters $a = b = 49.96$, $c = 103.20$ Å.

1. Introduction

The Na^+/H^+ exchangers (NHEs) are electroneutral transporters that catalyze the countertransport of Na^+ and H^+ through the plasma membrane and other intracellular organellar membranes in various animal species (Wakabayashi *et al.*, 1997; Orlowski & Grinstein, 2004). Nine different NHE isoforms (NHE1–NHE9) have been identified in mammalian tissues. Although they have been shown to exhibit similar membrane topology, these isoforms are thought to play different roles in various tissues (Counillon & Pouysségur, 2000; Orlowski & Grinstein, 2004). The isoform NHE1 is ubiquitously expressed in all tissues and cell types and plays a major role in maintaining intracellular pH and cell-volume homoeostasis (Putney *et al.*, 2002). The activity of NHE1 is controlled by various extrinsic factors, including growth factors, hormones and mechanical stimuli (Wakabayashi *et al.*, 1997; Counillon & Pouysségur, 2000; Orlowski & Grinstein, 2004). NHE1 is regulated by a variety of signalling molecules including calcineurin B homologous protein (CHP; Lin & Barber, 1996; Pang *et al.*, 2001) and Ca^{2+}/calmodulin (Bertrand *et al.*, 1994; Wakabayashi *et al.*, 1994). Despite intensive studies on NHE1 and its regulation, structural information is extremely limited, especially for the cytoplasmic C-terminal domain which contains most of the binding domains for the regulatory proteins.

CHP was initially identified as a protein (p22) involved in vesicular transport (Barroso *et al.*, 1996) and also as a molecule that interacts with NHE (Lin & Barber, 1996). CHP has also been reported to be involved in various cell functions, such as inhibition of calcineurin phosphatase activity (Lin *et al.*, 1999) and interaction with microtubules (Timm *et al.*, 1999), DRAK2 (death-associated protein kinase-related apoptosis-inducing protein kinase 2; Matsumoto *et al.*, 2001) and KIF1Bβ2 (kinesin family 1Bb2; Nakamura *et al.*, 2002). We have previously reported that CHP is an essential cofactor for supporting the physiological activity of the Na^+/H^+ exchanger by interacting with its juxtamembrane cytoplasmic domain (Pang *et al.*, 2001). Furthermore, we demonstrated that in contrast to the ubiquitous CHP1 isoform, CHP2 (61% amino-acid identity with CHP1) is highly expressed in malignantly transformed cells and may be involved in maintaining the high intracellular pH (pH_i) in cancer cells (Pang *et al.*, 2002). NHE1 mutants lacking the CHP-binding region (amino acids 515–530) exhibited low exchange activity (5–10% of the wild-type level; Pang *et al.*, 2001), suggesting that this region is essential for normal exchange activity of NHE1. This region with bound CHP would therefore function as a key structure maintaining the physiologically active conformation of NHE1 (Pang *et al.*, 2001).

Table 1
Data-collection statistics.

Values in parentheses are for the highest resolution shell (2.8–2.7 Å).

X-ray source	SPring-8 BL41XU
Space group	$P4_1$ or $P4_3$
Unit-cell parameters (Å, °)	$a = b = 49.96$, $c = 103.20$, $\alpha = \beta = \gamma = 90$
Wavelength (Å)	1.0000
Resolution range (Å)	50.00–2.70 (2.80–2.70)
Total reflections	26984
Unique reflections	6807
$R_{\rm merge}$† (%)	4.8 (25.1)
Completeness (%)	97.3 (83.1)
$\langle I/\sigma(I)\rangle$	17.3 (4.5)
Redundancy	4.0 (3.1)
Crystal mosaicity (°)	0.458

† $R_{\rm merge} = \sum_{hkl}\sum_i |I_i(hkl) - \langle I(hkl)\rangle| / \sum_{hkl}\sum_i I_i(hkl)$, where $I_i(hkl)$ is the ith intensity measurement of reflection hkl and $\langle I(hkl)\rangle$ is its average.

ADSC Quantum 315 CCD detector installed on the BL41XU beamline at SPring-8. The data collection was performed at a wavelength of 1.000 Å over a total range of 180°, with individual frames of 1° and an exposure time of 4 s. The crystal-to-detector distance was 350 mm. The collected images were processed using *HKL*2000 (Otwinowski & Minor, 1997).

3. Results and discussion

CHP is an important regulatory factor that maintains the physiologically active conformation of NHE1. In this study, in order to clarify the regulatory mechanism of NHE1 by CHP, we coexpressed CHP2 and its binding domain in NHE1 (amino acids 503–545) in *E. coli* and crystallized the complex. Firstly, we confirmed that the purified complex CHP2–NHE1-peptide was retained as a single peak on gel-filtration chromatography, indicating that the stable complex exists as a monomer (M_r = 28 000) in solution. In addition, using a 4–12% polyacrylamide gradient gel we confirmed that the purity of the complex is suitable for crystallization assay and that the purified sample contained equimolar amounts (1:1 molar ratio) of CHP2 and NHE1-peptide (Fig. 1).

Crystals suitable for X-ray crystallographic analysis were obtained within 2–3 d at 293 K using the sitting-drop vapour-diffusion method (Fig. 2). A previous attempt to collect crystallographic data at beamline BL44B2 (SPring-8) gave a maximum resolution of 3.0 Å owing to the small size of crystals. To obtain higher resolution data, we used the undulator beamline BL41XU. Crystals diffracted to 2.5 Å resolution along the c axis of the crystal, but the data set was only qualitatively useful to 2.7 Å because of anisotropic diffraction.

The tetragonal crystal of CHP2–NHE1-peptide was determined to be $P4_1$ or $P4_3$, with unit-cell parameters $a = b = 49.96$, $c = 103.20$ Å. Assuming the presence of one CHP2–NHE1-peptide complex molecule in the asymmetric unit, the Matthews coefficient V_M was calculated to be 2.5 Å^3 Da^{-1}, indicating a solvent content of approximately 49.5% in the unit cell. These values are within the typical range for protein crystals (Matthews, 1968).

The native data set has 6807 unique reflections, giving a data-set completeness of 97.3% in the resolution range 50.0–2.7 Å, with an $R(I)_{\rm merge}$ of 4.8% (Table 1). Although CHP2 shows about 36% sequence identity with human CNB (PDB code 1aui; Kissinger *et al.*, 1995), molecular replacement using CNB as a search model with *MOLREP* (Vagin & Teplyakov, 1997) was unsuccessful. Further crystallization refinement and structural analysis by multi-wavelength anomalous dispersion methods using selenomethionine and also taking advantage of the presence of yttrium as an additive are in progress.

We thank the staff at beamlines BL44B2 and BL41XU, SPring-8 for data-collection support and Dr Tianxiang Pang for initial participation in this study. This work was supported by grant Nano-001 for Research on Advanced Medical Technology from the Ministry of Health, Labour and Welfare of Japan and Grant-in-Aid for Priority Areas 13142210 for Scientific Research from the Ministry of Education, Science and Culture of Japan. YBA was supported by a Japan Society for the Promotion of Science (JSPS) Postdoctoral Fellowship.

References

Barroso, M. R., Bernd, K. K., DeWitt, N. D., Chang, A., Mills, K. & Sztul, E. S. (1996). *J. Biol. Chem.* **271**, 10183–10187.
Bertrand, B., Wakabayashi, S., Ikeda, T., Pouysségur, J. & Shigekawa, M. (1994). *J. Biol. Chem.* **269**, 13703–13709.
Counillon, L. & Pouysségur, J. (2000). *J. Biol. Chem.* **275**, 1–4.
Kissinger, C. R., Parge, H. E., Knighton, D. R., Lewis, C. T., Pelletier, L. A., Tempczyk, A., Kalish, V. J., Tucker, K. D., Showalter, R. E., Moomaw, E. W., Gastinel, L. N., Habuka, N., Chen, X., Maldonado, F., Barker, J. E., Bacquet, R. & Villafranca, J. E. (1995). *Nature (London)*, **378**, 641–644.
Lin, X. & Barber, D. L. (1996). *Proc. Natl Acad. Sci. USA*, **93**, 12631–12636.
Lin, X., Sikkink, R. A., Rusnak, F. & Barber, D. L. (1999). *J. Biol. Chem.* **274**, 36125–36131.
Matsumoto, M., Miyake, Y., Nagita, M., Inoue, H., Shitakubo, D., Takemoto, K., Ohtsuka, C., Murakami, H., Nakamura, N. & Kanazawa, H. (2001). *J. Biochem.* **130**, 217–225.
Matthews, B. W. (1968). *J. Mol. Biol.* **33**, 491–497.
Nakamura, N., Miyake, Y., Matsushita, M., Tanaka, S., Inoue, H. & Kanazawa, H. (2002). *J. Biochem.* **132**, 483–491.
Orlowski, J. & Grinstein, S. (2004). *Pflugers Arch.* **447**, 549–565.
Otwinowski, Z. & Minor, W. (1997). *Methods Enzymol.* **276**, 307–326.
Pang, T., Hisamitsu, T., Mori, H., Shigekawa, M. & Wakabayashi, S. (2004). *Biochemistry*, **43**, 3628–3636.
Pang, T., Su, X., Wakabayashi, S. & Shigekawa, M. (2001). *J. Biol. Chem.* **276**, 17367–17372.
Pang, T., Wakabayashi, S. & Shigekawa, M. (2002). *J. Biol. Chem.* **277**, 43771–43777.
Putney, L. K., Denker, S. P. & Barber, D. L. (2002). *Annu. Rev. Pharmacol. Toxicol.* **42**, 527–552.
Timm, S., Titus, B., Bernd, K. & Barroso, M. (1999). *Mol. Biol. Cell*, **10**, 3473–3488.
Vagin, A. A. & Teplyakov, A. (1997). *J. Appl. Cryst.* **30**, 1022–1025.
Wakabayashi, S., Bertrand, B., Ikeda, T., Pouysségur, J. & Shigekawa, M. (1994). *J. Biol. Chem.* **269**, 13710–13715.
Wakabayashi, S., Shigekawa, M. & Pouyssegur, J. (1997). *Physiol. Rev.* **77**, 51–74.

Consequently, more detailed structural information including the crystal structure of CHP complexed with its binding domain is of great importance to reveal the mechanism by which CHP is involved in this important regulation pathway of NHE1.

Here, we report the first crystallization and preliminary crystallographic studies of the human CHP2 complexed with the C-terminal cytoplasmic region (amino acids 503–545) of NHE1. Hereafter, the protein complex is referred to as CHP2–NHE1-peptide.

2. Materials and methods

2.1. Protein expression and purification

Human CHP2 cDNA (GenBank accession No. AF146019) corresponding to amino-acid residues 1–196 cloned into pET11 vector (Novagen) as a fusion protein with a C-terminal His_6 tag was co-expressed in *Escherichia coli* (BL21-Star; Invitrogen) with the human cDNA encoding the cytoplasmic binding-domain region of NHE1 peptide cloned into pET24 vector (Novagen). Six histidine residues were inserted after Lys196 of CHP2, while a stop codon was incorporated just after the sequence coding for the NHE1 peptide to eliminate the His_6 tag from the vector. Using this coexpression system, as also described previously for CHP1 (Pang *et al.*, 2004), we were able to obtain CHP2 in a complex form with its binding domain of NHE1. Cells were cultured in 2×YT medium containing 100 μg ml^{-1} ampicillin and 100 μg ml^{-1} kanamycin at 310 K. At an optical density of 0.6 at 600 nm, protein expression was induced by the addition of IPTG to a final concentration of 1 m*M* and cells were grown overnight at 291 K. The cells were harvested and resuspended in PBS buffer containing 1 m*M* phenylmethylsulfonyl fluoride (PMSF) and disrupted by sonication at 277 K. After centrifugation at 277 K, the supernatant containing the complex CHP2–NHE1-peptide was applied onto an Ni–NTA agarose affinity column (Invitrogen) equilibrated with PBS buffer. The column was washed with buffer *A* (20 m*M* sodium phosphate, 500 m*M* NaCl and 2 *M* KCl pH 6.0), buffer *B* (20 m*M* sodium phosphate and 500 m*M* NaCl pH 4.7) and then buffer *C* (20 m*M* sodium phosphate and 500 m*M* NaCl pH 6.0). The adsorbed protein complex was eluted with buffer *C* containing 500 m*M* imidazole, dialyzed overnight against buffer *D* (20 m*M* Tris–HCl pH 8.5) and further purified using a DEAE-Sepharose column (HiTrap DEAE FF 5 ml; Amersham Biosciences) eluted with a gradient from 0 to 1 *M* NaCl in 20 m*M* Tris–HCl buffer pH 8.5. A final purification step was carried out using gel-filtration chromatography (Superdex 200; Amersham Bioscience). The gel-filtration column was eluted with a buffer solution containing 100 m*M* NaCl and 20 m*M* Tris–HCl pH 7.5. The fraction containing CHP2–NHE1-peptide was pooled, dialyzed against 20 m*M* Tris–HCl pH 7.5, concentrated (20–25 mg ml^{-1}) using Amicon Ultra (Millipore) and subjected to crystallization without removing the His_6 tag.

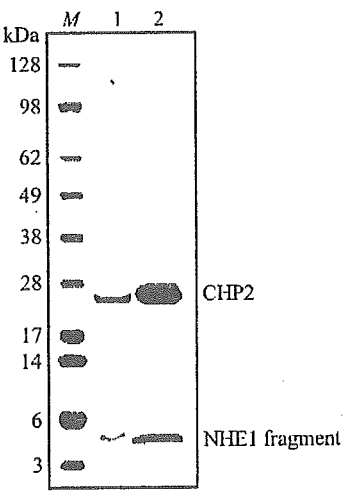

Figure 1
Polyacrylamide gel-electrophoresis pattern of the complex CHP2–NHE1-peptide. Crystals were collected and washed with the cryoprotectant solution. Collected crystals and 10 μg of the purified complex were applied to 4–12% gradient gel for lanes 1 and 2, respectively. Proteins were stained with Coomassie Brilliant Blue.

2.2. Crystallization

Preliminary screening of crystallization conditions was performed using various commercial kits (Hampton Research Crystal Screen kits, Emerald BioSystems Screen kits, Sigma–Aldrich Crystallization kits) and carried out using the sitting-drop vapour-diffusion method at 293, 287 and 277 K. 1 μl aliquots of protein-complex solution (20–25 mg ml^{-1}) were mixed with 1 μl reservoir solution to form the droplet, which was equilibrated against 100 μl reservoir solution. The initial screening, involving about 1440 individual trials, was unsuccessful. Additives from Hampton Research were used together with the above screening kits in a second trial involving about 4320 individual trials and very small and thin needle-shape crystals were finally obtained with a crystallization solution containing 200 m*M* ammonium acetate, 100 m*M* Bis-Tris pH 5.5, 25%(*w*/*v*) polyethylene glycol 3350 (PEG 3350) and 5 m*M* yttrium chloride as an additive at 277 K. Refinement of the crystallization conditions to 200 m*M* ammonium acetate, 100 m*M* Bis-Tris pH 5.5, 25%(*w*/*v*) PEG 3350 and 10 m*M* yttrium chloride at 293 K improved the size of the crystals. The resultant crystals are mostly in clusters, with the occasional appearance of single crystals. Single crystals or dissected parts from the clusters were used for data collection.

2.3. Crystallographic data collection

Prior to data collection, single crystals were soaked in a solution containing 200 m*M* ammonium acetate, 100 m*M* Bis-Tris pH 5.5, 35%(*w*/*v*) PEG 3350 and 10 m*M* yttrium chloride and flash-frozen under a nitrogen flow at 100 K. The crystals were evaluated in-house with Cu $K\alpha$ radiation (λ = 1.5418 Å) generated by an RA-Micro 7 rotating-anode X-ray generator with R-AXIS VII imaging-plate detector (Rigaku). High-resolution data sets were collected using an

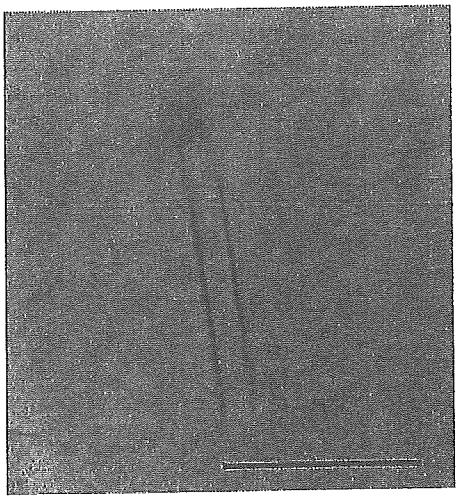

Figure 2
Crystal of human CHP2–NHE1-peptide as grown by the sitting-drop method. The scale bar indicates 0.1 mm.

Table 1
Data-collection statistics.

Values in parentheses are for the highest resolution shell (2.8–2.7 Å).

X-ray source	SPring-8 BL41XU
Space group	$P4_1$ or $P4_3$
Unit-cell parameters (Å, °)	$a = b = 49.96$, $c = 103.20$, $\alpha = \beta = \gamma = 90$
Wavelength (Å)	1.0000
Resolution range (Å)	50.00–2.70 (2.80–2.70)
Total reflections	26984
Unique reflections	6807
$R_{\rm merge}$† (%)	4.8 (25.1)
Completeness (%)	97.3 (83.1)
$\langle I/\sigma(I)\rangle$	17.3 (4.5)
Redundancy	4.0 (3.1)
Crystal mosaicity (°)	0.458

† $R_{\rm merge} = \sum_{hkl}\sum_i |I_i(hkl) - \langle I(hkl)\rangle| / \sum_{hkl}\sum_i I_i(hkl)$, where $I_i(hkl)$ is the ith intensity measurement of reflection hkl and $\langle I(hkl)\rangle$ is its average.

ADSC Quantum 315 CCD detector installed on the BL41XU beamline at SPring-8. The data collection was performed at a wavelength of 1.000 Å over a total range of 180°, with individual frames of 1° and an exposure time of 4 s. The crystal-to-detector distance was 350 mm. The collected images were processed using *HKL*2000 (Otwinowski & Minor, 1997).

3. Results and discussion

CHP is an important regulatory factor that maintains the physiologically active conformation of NHE1. In this study, in order to clarify the regulatory mechanism of NHE1 by CHP, we coexpressed CHP2 and its binding domain in NHE1 (amino acids 503–545) in *E. coli* and crystallized the complex. Firstly, we confirmed that the purified complex CHP2–NHE1-peptide was retained as a single peak on gel-filtration chromatography, indicating that the stable complex exists as a monomer (M_r = 28 000) in solution. In addition, using a 4–12% polyacrylamide gradient gel we confirmed that the purity of the complex is suitable for crystallization assay and that the purified sample contained equimolar amounts (1:1 molar ratio) of CHP2 and NHE1-peptide (Fig. 1).

Crystals suitable for X-ray crystallographic analysis were obtained within 2–3 d at 293 K using the sitting-drop vapour-diffusion method (Fig. 2). A previous attempt to collect crystallographic data at beamline BL44B2 (SPring-8) gave a maximum resolution of 3.0 Å owing to the small size of crystals. To obtain higher resolution data, we used the undulator beamline BL41XU. Crystals diffracted to 2.5 Å resolution along the c axis of the crystal, but the data set was only qualitatively useful to 2.7 Å because of anisotropic diffraction.

The tetragonal crystal of CHP2–NHE1-peptide was determined to be $P4_1$ or $P4_3$, with unit-cell parameters $a = b = 49.96$, $c = 103.20$ Å. Assuming the presence of one CHP2–NHE1-peptide complex molecule in the asymmetric unit, the Matthews coefficient V_M was calculated to be 2.5 Å^3 Da^{-1}, indicating a solvent content of approximately 49.5% in the unit cell. These values are within the typical range for protein crystals (Matthews, 1968).

The native data set has 6807 unique reflections, giving a data-set completeness of 97.3% in the resolution range 50.0–2.7 Å, with an $R(I)_{\rm merge}$ of 4.8% (Table 1). Although CHP2 shows about 36% sequence identity with human CNB (PDB code 1aui; Kissinger *et al.*, 1995), molecular replacement using CNB as a search model with *MOLREP* (Vagin & Teplyakov, 1997) was unsuccessful. Further crystallization refinement and structural analysis by multi-wavelength anomalous dispersion methods using selenomethionine and also taking advantage of the presence of yttrium as an additive are in progress.

We thank the staff at beamlines BL44B2 and BL41XU, SPring-8 for data-collection support and Dr Tianxiang Pang for initial participation in this study. This work was supported by grant Nano-001 for Research on Advanced Medical Technology from the Ministry of Health, Labour and Welfare of Japan and Grant-in-Aid for Priority Areas 13142210 for Scientific Research from the Ministry of Education, Science and Culture of Japan. YBA was supported by a Japan Society for the Promotion of Science (JSPS) Postdoctoral Fellowship.

References

Barroso, M. R., Bernd, K. K., DeWitt, N. D., Chang, A., Mills, K. & Sztul, E. S. (1996). *J. Biol. Chem.* **271**, 10183–10187.
Bertrand, B., Wakabayashi, S., Ikeda, T., Pouysségur, J. & Shigekawa, M. (1994). *J. Biol. Chem.* **269**, 13703–13709.
Counillon, L. & Pouysségur, J. (2000). *J. Biol. Chem.* **275**, 1–4.
Kissinger, C. R., Parge, H. E., Knighton, D. R., Lewis, C. T., Pelletier, L. A., Tempczyk, A., Kalish, V. J., Tucker, K. D., Showalter, R. E., Moomaw, E. W., Gastinel, L. N., Habuka, N., Chen, X., Maldonado, F., Barker, J. E., Bacquet, R. & Villafranca, J. E. (1995). *Nature (London)*, **378**, 641–644.
Lin, X. & Barber, D. L. (1996). *Proc. Natl Acad. Sci. USA*, **93**, 12631–12636.
Lin, X., Sikkink, R. A., Rusnak, F. & Barber, D. L. (1999). *J. Biol. Chem.* **274**, 36125–36131.
Matsumoto, M., Miyake, Y., Nagita, M., Inoue, H., Shitakubo, D., Takemoto, K., Ohtsuka, C., Murakami, H., Nakamura, N. & Kanazawa, H. (2001). *J. Biochem.* **130**, 217–225.
Matthews, B. W. (1968). *J. Mol. Biol.* **33**, 491–497.
Nakamura, N., Miyake, Y., Matsushita, M., Tanaka, S., Inoue, H. & Kanazawa, H. (2002). *J. Biochem.* **132**, 483–491.
Orlowski, J. & Grinstein, S. (2004). *Pflugers Arch.* **447**, 549–565.
Otwinowski, Z. & Minor, W. (1997). *Methods Enzymol.* **276**, 307–326.
Pang, T., Hisamitsu, T., Mori, H., Shigekawa, M. & Wakabayashi, S. (2004). *Biochemistry*, **43**, 3628–3636.
Pang, T., Su, X., Wakabayashi, S. & Shigekawa, M. (2001). *J. Biol. Chem.* **276**, 17367–17372.
Pang, T., Wakabayashi, S. & Shigekawa, M. (2002). *J. Biol. Chem.* **277**, 43771–43777.
Putney, L. K., Denker, S. P. & Barber, D. L. (2002). *Annu. Rev. Pharmacol. Toxicol.* **42**, 527–552.
Timm, S., Titus, B., Bernd, K. & Barroso, M. (1999). *Mol. Biol. Cell*, **10**, 3473–3488.
Vagin, A. A. & Teplyakov, A. (1997). *J. Appl. Cryst.* **30**, 1022–1025.
Wakabayashi, S., Bertrand, B., Ikeda, T., Pouysségur, J. & Shigekawa, M. (1994). *J. Biol. Chem.* **269**, 13710–13715.
Wakabayashi, S., Shigekawa, M. & Pouyssegur, J. (1997). *Physiol. Rev.* **77**, 51–74.